Quantification of prognostic parameters for assessment of diabetes-related foot ulcers and venous leg ulcers using image processing techniques

A thesis submitted in fulfilment of the requirements for the degree of Doctor of Philosophy

Priya Rani

M.S. (By Research)

VIT University, India

School of Engineering

College of Science, Engineering and Health

RMIT University

August 2019

Declaration

I certify that except where due acknowledgement has been made, the work is that of the author alone; the work has not been submitted previously, in whole or in part, to qualify for any other academic award; the content of the thesis is the result of work which has been carried out since the official commencement date of the approved research program; any editorial work, paid or unpaid, carried out by a third party is acknowledged; and, ethics procedures and guidelines have been followed.

Priya Rani

23/08/2019

Acknowledgements

I would like to thank my senior supervisor, Prof. Dinesh Kant Kumar for his inspiring ideas, constant support and excellent guidance during my research. I would also like to sincerely thank my associate supervisors, Dr. Behzad Aliahmad and Dr. P. J. Radcliffe for their inspiring ideas, support and guidance throughout my candidature. My supervisors constantly motivated and helped in building up my self-confidence to do good and innovative work.

I would like to thank the research fellows in the Bio-signals lab, Dr. Sridhar Arjunan and Dr. Hao Hao for their valuable feedback and suggestions on my work. I would also like to thank Dr. Rajna Ogrin and Jacinta Anderson of Bolton Clarke, Melbourne for sharing the clinical database and for providing valuable clinical suggestions and feedback on the work. I would also like to thank the team at Austin Hospital, Melbourne for sharing the clinical database for my work.

My heartfelt thanks to my colleagues in the Bio-signals lab, Adrian, Rekha, Susmit, Parham, Aqsa and Sana for providing their help and support throughout my candidature and making research life easy with fun and laughter. I would also like to thank all my friends at RMIT University for their support and encouragement during my research study.

I would like to express my deepest gratitude and love to my parents, Mr. Ramesh Prasad and Mrs. Madhuri Kumari and my sister Manisha for their unconditional love, support and encouragement during my research.

Last but not the least, I would like to thank the staff members of School of Engineering, RMIT University, Australia for their unsparing dedication and continuous support.

Abstract

Diabetes-related Foot Ulcers (DFUs) and Venous Leg Ulcers (VLUs) are two important types of chronic wounds which do not heal in an orderly fashion and being a major cause of morbidity in extreme cases. Assessment of these ulcers is a growing concern among health care professionals across the globe. Currently, healing of these ulcers is assessed by monitoring the changes in their area over four consecutive weeks. The suggested clinical monitoring parameter is that the ulcers which show more than fifty percent reduction in the area by week four (after the ulcers are reported in the clinics) are predicted to heal within twelve weeks of time. However, this is a subjective measurement, performed manually using a ruler; based on the assumption that the ulcer is purely rectangular. Moreover, the above-mentioned monitoring method fails to work in most of the cases, as healing of these ulcers is a complicated, multi-factorial process which cannot be assessed only by a single parameter (i.e., area).

This research work has proposed new objective parameters for assessment and prediction of these ulcers by studying the shape of the ulcers, temperature distribution of the ulcer and on the ulcerated foot and area measurement of the ulcers using different techniques. This work has also examined the association of the proposed parameters with patient's clinical information, etiological factors and the healing status of the ulcers. Literature has suggested that there is a change in the irregularity of the ulcers as they heal, thus, playing the role in the healing of the ulcers. Based on this fact, this work hypothesized that the edges of the ulcers can be assessed by quantifying the change in irregularity in them. The widely used technique of measurement of irregularity is Fractal Dimension (FD). However, FD has the limitation of inherent limited resolution of the digitized images, which renders these images as non-fractal, as the self-similarity properties of the images are lost. Thus, this work proposed a new index measure and developed an algorithm for measurement of irregularity and tested it on synthetic images initially. The new index measure called curve irregularity index (I_c) measures the change in the irregularity of the segments of the contours with change in window sizes and does not assume the objects to have self-similar properties. The I_c was then measured and validated on the contours of DFUs and VLUs and the association of irregularity of the contours with etiological factors and the healed status of the ulcers, respectively, was reported. This work has employed the normal DSLR camera and digital planimetry technique to capture the

RGB images and to obtain the tracings of the ulcers respectively. This work has shown the significance of contour irregularity of ulcers with the clinical conditions of patients and differentiated between the healed and not-healed ulcers.

This research has also employed infrared thermal imaging technique to obtain the temperature distribution of the ulcers. Literature has reported the association of temperature with the risk of ulceration in neuropathic and ischemic conditions of the feet. However, very few works have been done on the study of temperature of the existing ulcers. Hence, this work tested and obtained the association of the mean temperature of the DFUs with the clinical conditions of the participants. This work also hypothesized that the area obtained based on thermal distribution can differentiate between the healed and not-healed ulcers in VLUs. Hence, segmentation of the ulcer region from the thermal images was performed based on an active contour model, previously developed for segmentation of contours in images where edges are not defined by gradient. The obtained results showed that the area thus obtained from the ulcer regions of all five weeks showed association with the healed status of the VLUs and can differentiate between the healed and not-healed ulcers. This work can also be used to predict the healing trajectory of the ulcers. Thus, the overall research work would find application in the clinical set ups to aid in the assessment and prediction of the healing status of DFUs and VLUs and would lead to provide better health-related quality of lives to the patients.

Publications Arising From This Thesis

Fully Refereed International Journals

1. **Rani, P**, Aliahmad, B & Kumar, DK 2019, 'Curve irregularity index for quantification of roughness in non-fractal curves', *Physica A: Statistical Mechanics and its Applications*, vol. 528, p. 121435.

2. Aliahmad, B, Tint, AN, Poosapadi Arjunan, S, **Rani, P**, Kumar, DK, Miller, J, Zajac, JD, Wang, G & Ekinci, EI 2018, 'Is Thermal Imaging a Useful Predictor of the Healing Status of Diabetes-Related Foot Ulcers? A Pilot Study', *Journal of diabetes science and technology*, vol., p. 1932296818803115.

Fully Refereed Conference Proceedings

1. **Rani, P**, Aliahmad, B. and Kumar, D.K., 2017, July, 'A novel approach for quantification of contour irregularities of diabetic foot ulcers and its association with ischemic heart disease' In *2017 39th Annual International Conference of the IEEE Engineering in Medicine and Biology Society (EMBC)* (pp. 1437-1440). IEEE.

2. **Rani, P**, Aliahmad, B & Kumar, DK 2019, July, 'The association of temperature of Diabetic Foot Ulcers with Chronic Kidney Disorder ', In *2019 41st Annual International Conference of the IEEE Engineering in Medicine and Biology Society (EMBC)*. IEEE.

Contents

List of Figures

List of Tables

Chapter 1

Introduction

1.1 Introduction

Diabetes-related foot ulcers (DFUs) and venous leg ulcers (VLUs) are important chronic wounds, primarily because they do not heal in an orderly fashion and within the predictable time frame. DFUs frequently occur in people with diabetes due to damage and injury to the feet, mainly due to the loss of sensation in the feet. VLUs occur in elderly people and are mainly caused due to venous obstruction or reflux, leading to poor return of blood. Both types of ulcers are a major cause of morbidity, with associated risk of infection, amputation and mortality.

Assessment of these ulcers is a growing concern among health care professionals. Currently, healing of these ulcers is assessed by monitoring the changes in their surface area over four consecutive weeks. However, this is a subjective measurement, performed manually using a ruler; based on the assumption that the ulcer is purely rectangular, which is not a reliable method of measurement. Moreover, healing of these ulcers is a multi-factorial process and cannot be determined by a single subjective parameter. Managing these ulcers is a complicated process that requires simultaneous attention to maximizing blood supply, managing infection, wound debridement, ulcer dressings and pressure off-loading. Early and multi-disciplinary care of these ulcers is essential in preventing deterioration and the potential need for amputation. Thus, timely and tailored ulcer care is an important step in enhancing the healing process and must be taken seriously to reduce the overall impact on the patient (with respect to the duration and cost of treatment) and maximize ulcer healing. Thus, there is a need to have better prognostic parameters to help in the assessment of the healing of these ulcers.

Literature states that there are alternative objective ways of assessing the ulcers, such as complexity analysis of the contours of the ulcers and temperature distribution of the ulcers. Earlier works have shown that the temperature distribution and monitoring has been used as a preventative and predictive tool for outbreak of ulcers (Houghton, Bower & Chant 2013). It has also been stated that there is a change in the complexity of the ulcers as they heal, thus playing its role in the healing of ulcers (Rowledge et al. 2016). These parameters can be the alternate objective parameters which can aid in better assessment of the healing of ulcers.

1.2 Problem Statement

Best practice care of the ulcer involves diagnosing the etiology of the ulcer and developing a management plan that addresses the etiological factors with ongoing monitoring of healing (AWMA 2010). The most common location of ulcers in community members is in the lower leg and the foot, leading to venous leg ulcers or diabetes-related foot ulcers (Forssgren, Fransson & Nelzén 2008; O'Meara, Cullum & Nelson 2009). Normal healing constitutes a reduction in ulcer's area by 50% within 4 weeks of treatment and has been considered as the current clinical monitoring parameter for the assessment of ulcers (Cardinal et al. 2008). However, this technique worked positively for only 58% of the cases in diabetes-related foot ulcers cases (Khaodhiar et al. 2007). In case of venous leg ulcers, despite best practice management, over 20% of ulcers do not heal in the expected trajectory and may require additional interventions to improve outcomes (Coyer, Edwards & Finlayson 2005; Edwards, H et al. 2013). Hence these ulcers pose serious threats to the life of the patients, if they become chronic in nature.

Successful clinical management has the potential to improve the quality of life and the economical and functional burden of clinicians and patients affected with ulcers (Nouvong et al. 2009). Therefore, new techniques which are simple, inexpensive, user-friendly, real-time, portable and non-invasive, can provide immediate information with improved accuracy, sensitivity and specificity and can be of great help in the effective management of these ulcers. Two of the objective parameters reported in literature for the assessment of ulcers is change in the contour irregularity of ulcers and change in the temperature distribution of the ulcers and their surrounding regions. The commonly used method reported in literature for measurement of irregularity in contours is Fractal Dimension (FD). It has been used as an effective measure in description and characterization of irregularity in the biological tissues which show self-similar properties (Carbonetto & Lew 2010; Jayalalitha & Uthayakumar 2007). However, even with the assumption of ulcer contour being a fractal object and showing infinite repeatable pattern at every scale, the limitation in measurement of irregularity using FD comes with the inherent limited resolution of the digitized ulcer images, which renders them as non-fractal objects.

The second objective parameter is the temperature distribution of the ulcers. In the previous works, thermal imaging has been used as a preventive tool for the outbreak of ulcers and no works have been done on the assessment of open ulcers. Moreover, the limitation of the previous works is that contralateral foot has been used as a reference for prediction in the

ipsilateral foot, which fails if the contralateral foot also has potential of ulceration or already has ulcers on it. Another limitation is that the mean temperature of whole feet or few points on the feet have been taken for comparison with the contralateral foot, which can lead to wrong diagnosis, in case the feet are similarly hot/cold. Thus, this work has overcome these limitations and tested for new objective parameters on DFUs and VLUs to assist in better assessment of these ulcers.

1.3 Hypotheses

This research work has been conducted based on the following hypothesis:

Hypothesis 1: One of the important aspects considered for the assessment of ulcers are the ulcers' edges or contours; hence it is important to study the properties of ulcer contours of the healing and non-healing ulcers. Fractal Dimension has been widely used in the past to quantify the irregularity in biological objects, however, it fails to quantify contour irregularity in ulcers due to the inherent limited resolution of the digitized ulcer images. This work has hypothesized that the ulcer edge can be assessed by quantifying the changes in irregularity of the ulcer contour which is independent of the self-similarity properties of the ulcers.

Hypothesis 2: Existing literature on thermal imaging of ulcers is focused on the potential risk of ulceration and has been done for prediction of ulceration. The use of contralateral foot and consideration of mean temperature of whole foot limit the robustness of the studies. This work has hypothesized that the variation in temperature pattern in the ulcers shows association with the clinical conditions of the patients. It will focus on the assessment of existing ulcers and analysis of ulcerated foot will be done independently, without relying on the contralateral or non-ulcerated foot.

Hypothesis 3: Thermal imaging has not been considered to measure the area of the open ulcers in the previous works. It has also not been used to differentiate between the healing ulcers and the non-healing ulcers. Prediction of the healing trajectory of ulcers and to differentiate between the healing and non-healing ulcers is very important for clinicians to provide suitable treatment and care to the patients. Thus, this work has hypothesized that thermal imaging can differentiate between the healed and not-healed ulcers based on the area measured due to temperature variation and can predict the healing trajectory of the ulcers.

1.4 Research Aim and Objectives

This work aims to identify new objective parameters for robust and accurate assessment of the DFUs and VLUs. This work will investigate the properties of the ulcer contours by measuring the fractal dimension, shape deformity and irregularity by introducing a new irregularity measure. It will use recent imaging technologies including digital planimetry and thermal imaging to measure the area of the ulcers in a more objective manner and to study the association of variation in temperature distribution of the ulcers with the healing status of the ulcers.

The objectives of this research are:

- To study the properties of ulcer contours of DFUs and VLUs and their association with co-morbidities and the healed status respectively.
- To study the association of temperature distribution of DFUs with clinical conditions.
- To differentiate between the healed and not-healed VLUs by investigating their area measured using different techniques (digital planimetry and thermal imaging).

Successful completion of this work will provide new objective parameters obtained from different imaging techniques and will help clinicians to perform better diagnosis of the healing of the ulcers. It will also help in the prediction of healing of ulcers in their early stages. If patients will be provided with a realistic estimate of their chances of healing within a set time, it may even increase the likelihood of their compliance with treatment. This will lead to successful diagnosis and management of DFUs and VLUs which will, in turn, reduce the cost of caring of patients to hospitals and will lead to elimination of secondary complications such as infection of ulcers and amputation of limbs, thus providing a better quality of life to the patients.

1.5 Outline of the Thesis

The thesis on this research work has been divided into eight chapters.

Chapter 1 gives an introduction of the research work and a brief on the limitations of the current techniques and clinical practices in the assessment of the healing status of diabetes-related foot ulcers and venous leg ulcers.

Chapter 2 provides a detailed description of the two diseases on which the study has been conducted- Diabetes-related foot ulcers and Venous leg ulcers. It also addresses the techniques and methods used for the assessment of these ulcers.

Chapter 3 introduces a novel approach to quantify the irregularity in the curves (such as ulcer contours) which do not show fractal characteristics. A comparative study with the current technique of fractal dimension has also been presented.

Chapter 4 introduces another novel approach to quantify the irregularity in non-fractal curves, more efficient than the one presented in previous chapter. It also includes the validation of the method on diabetes-related foot ulcers' contours and venous leg ulcers' contours.

Chapter 5 describes the use of Chan-Vese segmentation model for segmentation of the ulcer region from the thermal images of diabetes-related foot ulcers and shows the association of clinical conditions with the temperature of the ulcers.

Chapter 6 presents the use of digital planimetry technique and thermal imaging for measurement of area and shows the efficacy of the two methods in the prediction of the healing trajectory of venous leg ulcers.

Chapter 7 presents the conclusion of this research work and discusses the main contributions of this work in the clinical field.

Chapter 2

Literature review

2.1 Introduction

Chronic wounds are wounds which do not heal in an orderly fashion and in the predicted amount of time as other wounds. This chapter provides a description of two types of chronic wounds studied in this research work- *diabetes-related foot ulcers* and *venous leg ulcers*. The review in this chapter covers three major research areas:

- Diabetes-related foot ulcers- etiological factors and clinical intervention
- Venous leg ulcers- etiological factors and clinical intervention
- Current assessment techniques- strengths and limitations

Section 2.2 of the chapter describes diabetes-related foot ulcers, its statistics in Australia and around the globe along with the financial and social impact on the hospitals and the patients. It also covers the etiological factors and clinical interventions practiced by the clinicians. *Section 2.3* describes the second type of chronic ulcers- mixed venous leg ulcers, its statistical distribution, etiological factors and the clinical interventions. *Section 2.4* describes the current assessment techniques being used for the assessment of the healing status of the ulcers which includes area measurement, temperature measurement and oxygen saturation measurement of the ulcers. *Section 2.5* addresses the limitations of these techniques, thus emphasizing on the need for better diagnostic and predictive tools for assessment of these ulcers. Finally, *section 2.6* summarises all the above points and lists the research works being proposed in this study.

2.2 Diabetes-related foot ulcers

Diabetes mellitus (commonly referred to as Diabetes) is a chronic condition which is characterised by increased blood sugar concentration. It has been coined as the 'Black Death of the 21st century' due to its high similarities with the plague of 14th century in terms of high global prevalence, high morbidity and mortality (Lazzarini et al. 2012). The International Diabetes Federation (IDF) estimated that the global prevalence of diabetes based on the latest data available was 194 million in 2003, 285 million in 2009 and 382 million in 2013 (Ogurtsova

et al. 2017). It was also estimated that this number rose to 415 million worldwide in 2015 and would rise to 642 million by 2040 (Ogurtsova et al. 2017).

The main concern in people affected with Diabetes is that they have one or more diseases co-occurring with it (also called co-morbid diseases) (Yazdanpanah, Nasiri & Adarvishi 2015). Diabetes-related foot ulceration (DFU) is one of the common foot complications in patients suffering from Diabetes. Feet of a diabetic patient is more susceptible to damage and injury, mainly due to loss of sensation, and involves a break in the skin causing an ulcer, which extends through the dermis layer and may affect the underlying structural tissues (Reiber et al. 1999). It is estimated that 15% to 25% of patients suffering from type 1 and type 2 diabetes are at the risk of developing a foot ulcer during their lifetime and is more common in those over 60 years of age (Liu et al. 2015; Nouvong et al. 2009; Shearman, C 2015). DFUs usually take a long time to heal, even after receiving standard medication and care. One of the common outcomes of these ulcers is lower limb amputations and is reported to be the cause of amputation in 84% of the cases (Reiber et al. 1999; Smith-Strøm et al. 2017). This occurs due to failure in healing of the primary ulcer, recurrent ulceration or chronic infection. Foot ulceration may be prevented in most patients with self-care, medical and footwear strategies (Reiber et al. 1999). Despite spreading clinical awareness of its prevention, it is estimated that almost 2-3% of the people affected with diabetes develop a foot ulcer every year in U.S. and 4-10% in U.K. (Abbott et al. 2002; Ramsey et al. 1999; Reiber et al. 1999). In Australia, there are about 10,000 admissions in the hospital per year for DFUs, with lower-limb amputation being a common outcome (Davis et al. 2006). The number of amputations in Australia has increased by 30% from 1998 to 2011 due to DFUs and is the second highest in the developed world (Lazzarini et al. 2012; Norman et al. 2016). Figure 2.1 shows an example of a diabetes-related foot ulcer from the dataset used in this study.

Figure 2.1: An example of a diabetes-related foot ulcer (image taken from dataset collected for this study)

The effect of diabetes on the health-related quality of life (HRQL) is high, but it is even worse for people with DFUs (Ribu et al. 2007; Yotsu et al. 2014). They have significantly lower HRQL and higher rates of depression compared to the general population and the people with diabetes having no foot complications (Moulik, Mtonga & Gill 2003; Ribu et al. 2007). Up to 84% of people have been reported to have a major impact of DFUs on their lives with reduced mobility, pain, anxiety and depression (Shearman, C 2015; Shearman, CP 2015). Among these, the inability to stand, walk or work are found to be the most important determinants. Apart from amputations and lower HRQL, the impact on mortality is also high. The mortality rate among these patients is reported to be increasing from 39% to 80% in the last five years (Armstrong, Boulton & Bus 2017; Moulik, Mtonga & Gill 2003).

Foot ulcers also have economic impacts; they are costly, not only to the patients, but also to healthcare systems - in terms of expenditure and resources to support hospital inpatients and outpatients being managed by primary care and community care services, which includes visits to hospitals, regular dressing changes, hospitalization, amputation and orthotics (Shearman, C 2015; Sheehan et al. 2003). One of the studies suggested that 25-50% of the costs of the inpatient diabetes care might be related to DFUs alone (Armstrong, Boulton & Bus 2017; Lazzarini et al. 2012). The cost of diabetic foot ulceration and amputation was estimated to be about USD10.9 billion in 2001 in the US Medicare system (Boulton et al. 2005). In Australia, the treatment of foot ulcers cost about AUD14,691 in total and amputations cost about AUD23,555 in total for the hospitals and pharmaceuticals (Lazzarini et al. 2012).

2.2.1 Etiological factors and clinical intervention

DFUs are generally classified as neuropathic ulcers, ischemic ulcers and neuro-ischemic ulcers (Bakker et al. 2012; Iraj et al. 2013). Although neuropathic ulcers remain the most common

type of foot ulcers, recent data suggest that ischaemic and neuro-ischaemic ulcers are on the rise and possess a higher risk of adverse outcomes (Ndip & Jude 2009). These occur usually due to two lower-extremity diseases- peripheral neuropathy and peripheral vascular disease (PVD) (Ylitalo, Sowers & Heeringa 2011). Neuropathic ulcers account for over 80% of the foot ulcers and occur because of impaired sensation in the lower extremities and are usually located over pressure sites, such as the plantar aspect of the foot or dorsal surface of the toes. Ulcer formation is promoted by killing pain sensation and pressure perception and is surrounded by hyperkeratosis (thickening of the outer layer of the skin), covering the ulcers completely (Piaggesi et al. 1998). Feet having neuropathic ulcers are usually warm and have intact pulses, compared to ischaemic ulcers where the feet might be cold, would lack pulses and would often be painful (Bakker et al. 2012). Ischaemic ulcers usually affect the toes or tips of the feet and are caused by trauma such as ill-fitting footwear (Edmonds & Foster 2006; Ndip & Jude 2009). Neuro-ischaemic ulcers possess a higher risk of adverse outcomes, as they occur in individuals with both neuropathy and ischemia (Ndip & Jude 2009). They are typical neuropathic ulcers, but they have insufficient blood supply to promote healing (Bakker et al. 2012). They are cool and pulseless, poorly perfused with red marks on the skin and can be commonly seen on the edges of the feet, tips of toes or back of the heels. DFUs often have high bacterial growth, hence having a significant risk of secondary bacterial infection, which can range in severity from cellulitis affecting superficial regions to deeper bony regions, which needs more rigorous treatment (Lipsky et al. 2012). In untreated or severe cases, DFUs progress to osteomyelitis, which makes amputation necessary (Ramsey et al. 1999). Figure 2.2 shows examples of a neuropathic ulcer, ischemic ulcer and neuro-ischemic ulcer.

(a)

(b)

(c)

Figure 2.2: Examples of (a) neuropathic ulcer (b) Ischemic ulcer (c) neuro-ischemic ulcer (images taken from dataset collected for this study)

Diabetes is a multi-organ systemic disease, which means that there can be additional disorders or diseases co-occurring with it (Yazdanpanah, Nasiri & Adarvishi 2015). These complications can be macrovascular and microvascular including heart attack, stroke, blindness, kidney failure, lower limb amputations, etc. (Lazzarini et al. 2012). Some of the common factors predisposing people with DFUs are trauma, presence of peripheral neuropathy, foot deformity and peripheral arterial disease (Delbridge et al. 1985; Reiber et al. 1999). Thus, healing of

DFUs is affected by etiological factors, co-morbid diseases, patients' demographic and clinical status. Hence a detailed clinical history of the patients is needed to carry out appropriate investigations and assessment of the ulcers. This includes (but not limited to) information on the duration of ulcer, previous ulceration, history of trauma, family history of ulceration, ulcer characteristics (site, pain, odour, and exudate or discharge), limb temperature, underlying medical conditions (duration and type of diabetes mellitus, peripheral vascular disease, ischaemic heart disease, cerebrovascular accident, neuropathy), previous venous or arterial surgery, history of smoking and medications (Nouvong et al. 2009; Shearman, C 2015).

Some of the important co-morbid diseases which have been reported to affect the healing and have been considered in this work are peripheral vascular disease (PVD), cardiovascular diseases such as ischemic heart disease (IHD) and kidney disorders such as chronic kidney disease (CKD) (Meloni et al. 2018; Otte, van Netten & Woittiez 2015; Tresierra-Ayala & Rojas 2017).

PVD is a circulatory condition in which the blood flow to the limbs is considerably reduced due to narrowing of blood vessels (due to plaque formation). Thus, reduced blood flow to the lower limbs causes delayed healing in these ulcers (Tresierra-Ayala & Rojas 2017). Any disease or damage to the heart's blood vessels, such as fatal myocardial infarction or coronary artery disease are considered as IHD. Research has shown that not only does the presence of IHD cause delay in the healing of the ulcers but leads to a high rate of mortality too (Meloni et al. 2018). CKD is characterized by the presence of impaired kidney function, which worsens with time, if left unattended. This condition cannot be completely cured and has been reported to show association with the healing of the ulcers and lower limb amputations (Otte, van Netten & Woittiez 2015). Thus, for effective management of the ulcers, these comorbidities must be accounted for.

Among the etiological factors mentioned above, peripheral neuropathy and peripheral arterial disease are the primary factors behind the development of DFUs (Boyko et al. 1999; Jeffcoate 2012; Zimny, Schatz & Pfohl 2002). Peripheral neuropathy can affect the peripheral motor, autonomic and sensory nerves- while motor neuropathy make the feet more susceptible to injury due to alteration in foot shape and weight distribution, autonomic neuropathy causes vasomotor and sudomotor (sweating) abnormalities, resulting in dry and cracked skin which are more susceptible to infection (Andersen 2012; Seah et al. 2014). Sensory neuropathy leads to reduced sensation in the feet resulting in unawareness among individuals of ulcers being

developed in the feet (Tesfaye et al. 2010). Individuals continue to walk and often injure the area because of the lack of pain and seek help only after the condition is well developed (Seah et al. 2014; Tesfaye et al. 2010). If the individual has peripheral arterial disease, the blood circulation to the legs is reduced, which compromises or prevents healing of the ulcer (Bakker et al. 2012; Seah et al. 2014). Other less robust predictors of risk of ulceration are age, gender and concurrent hypertension or dyslipidaemia (Seah et al. 2014).

Foot ulcers are treated by regular sharp debridement (surgical removal of dead tissues), applying appropriate dressings and off-loading of pressure away from the ulcers (Nouvong et al. 2009). It may include revascularization in cases of the presence of significant peripheral arterial disease and antibiotics, in cases of infection (Dumville et al. 2012; Laing 1998).

Although foot ulcers follow different courses before they heal completely, literature suggests that they should ideally heal within 8-12 weeks (Ince, Game & Jeffcoate 2007). The assessment of the ulcers includes subjective assessment of the odour, colour, exudates and the degree of inflammation in the surrounding region, and the more objective assessment of measurement of the size of the ulcer (Mani, Romanelli & Shukla 2012). Wound probing is also performed in certain cases to assess the depth of the ulcers and the infection in the ulcers using a suitable designed probe. This provides important information about the presence of diabetic foot osteomyelitis (Mani, Romanelli & Shukla 2012). Ideally, the volume of the ulcers should be measured to provide complete information about the healing; but this has practical limitations, since volume measurement is more complicated than area measurement (Pavlovčič et al. 2015). The change in the size of the ulcer over four consecutive weeks has been proven to be a good indicator to show the healing progress of the ulcers (Sheehan et al. 2003). Hence area measurement is considered as the reliable indicator of healing based on the assumption that the ulcer is rectangular (Mani, Romanelli & Shukla 2012). Figure 2.3 shows the images of four consecutive weeks of an ulcer which shows more than 50% reduction in the area from the baseline week.

(a) Week 1

(b) Week 2

(c) Week 3

(d) Week 4

Figure 2.3: An example of four weeks of an ulcer showing more than 50% reduction in its area by week 4 which healed completely by week 12 (images taken from dataset collected for this study)

A healed ulcer is defined as complete epithelialization of the skin and deemed healed by the treating podiatrist (Milne et al. 2013). Studies show that after providing standard wound care, ulcers which show 50 percent reduction in their area in 4 weeks, should heal completely at the end of 12 weeks (Coerper et al. 2009; Sheehan et al. 2003). Thus, the ulcers showing 50 percent reduction in the area at the end of 4 weeks have become the basic clinical monitoring parameter to distinguish the healing ulcers from the delayed healing ones. However, some ulcers fail to heal within this given time frame (Warriner, Snyder & Cardinal 2011; Zimny, Schatz & Pfohl 2002).

2.3 Venous leg ulcers

Chronic wounds are an under-recognised health issue in Australia, and hence there is limited data on the prevalence of these wounds. However, according to a recent review, the venous leg ulcers (VLUs) are the second most common type of chronic wounds after pressure injuries and comprise 12% of the total reported chronic wounds (Norman et al. 2016). Figure 2.4 shows the distribution of chronic wounds in hospitals and residential care settings in Australia. These are more common in elderly people and are a major cause of pain and disability (Ballard & Bergan

2012). They are chronic and recurring, with individuals suffering from open leg ulceration from a few weeks to 50 years (Briggs & Nelson 2010). They are caused by venous obstruction or reflux, which leads to poor venous return (poor return of blood from legs to the heart) and venous hypertension (increased pressure in the veins) (Nelson, Cullum & Jones 2006).

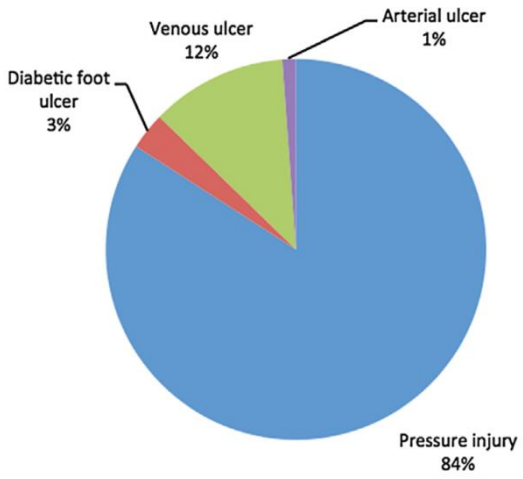

Figure 2.4: The distribution of chronic wounds in hospitals and residential care settings in Australia (Norman et al. 2016)

If economic burden is to be discussed, chronic wound treatment cost approximately USD15 billion per year in U.S. In Australia, the direct healthcare costs of these wounds are estimated to be at least USD2.85 billion per year to the health care systems, which includes costs in hospitals and residential care settings only (Norman et al. 2016). It is estimated that the older individuals with VLUs pay AUD27.5 million as out-of-pocket costs for consumables every year (Norman et al. 2016).

VLUs also reduce the HRQL and working capacity and increase social isolation in older people (Franks & Moffatt 2001; Price et al. 2008). Pain is a common feature of VLUs reported in literature; individuals with VLUs live with pain on a day-to-day basis, which affects normal everyday activities such as standing, walking, etc. These activities may even trigger the pain, thus having a major impact on both carers' and sufferers' quality of life, emotional state and sense of wellbeing (Briggs & Nelson 2010; Woo et al. 2008). Delayed healing of the ulcers also causes anxiety, fear of amputation, odour due to exudate leakage and isolation from society. These factors lead to depression in significant number of individuals (Jones et al. 2006). Pain and odour from the ulcers are two important ulcer-related symptoms which causes individuals to experience depression and anxiety as they are forced to stay at home to avoid

embarrassment (Fagervik-Morton & Price 2009; Nelson, Cullum & Jones 2006). The depressed individuals usually have disturbed sleep, poor appetite and self-neglect, which in turn, leads to delayed healing of the ulcers, thus making the mental wellbeing and healing of these chronic ulcers as co-dependent and associated factors (Jones et al. 2006). Hence these ulcers have a strong negative impact on the individuals' emotional state such as fear, anger, resentment and negative self-image (Phillips et al. 1994).

2.3.1 Etiological factors and clinical intervention

Venous ulcers are usually found in the gaiter area of the lower limb above the ankle joint. The skin and the subcutaneous tissue gets thickened and oedematous, with the surrounding regions having pigmentation and inflammation. They are serpiginous or oval and can be lateral, medial or circumferential in shape and location. The edges of these ulcers are usually flat and sloping. These ulcers never penetrate muscles and bone is never exposed (Savage 2012). Figure 2.5 shows the images of four weeks of a venous leg ulcer.

For the management of these ulcers, firstly, the details of the mode of onset and duration of the ulcers are noted. All demographic and clinical information of the patient's general health and past medical history are noted, as there can be multiple factors associated with the healing of these ulcers (Savage 2012). Some of the important wound components to be considered are site, duration, area, current use of antibiotic, ankle range of motion, ABPI (ankle brachial pressure index), etc. Ankle brachial pressure index (ABPI) is considered to be an important parameter in the assessment of VLUs and is measured using doppler ultrasound (Mani, Romanelli & Shukla 2012). ABPI is the ratio of the systolic blood pressure of the arm (ipsilateral brachial artery) and the ankle (posterior tibial artery). In a normal person, the pressure at the ankle is slightly higher than that of the arm, and a range of 0.91-1.3 is generally considered as normal arterial blood supply (Mani, Romanelli & Shukla 2012). The treatment of these ulcers is given by regular cleansing and debridement (if necessary), providing appropriate dressings, bandages, compression stockings and effective compression therapy for the ulcers to heal early (Briggs & Nelson 2010; Jones et al. 2006).

The monitoring of VLUs follows the same clinical parameter as that of DFUs as both these ulcers are classified as chronic wounds (Cardinal et al. 2008; Norman et al. 2016). They are monitored over several weeks by manually tracing the area of the ulcers and by performing subjective analysis of ulcer characteristics and the surrounding tissues, type of tissue of the wound bed and exudates produced over weeks. The progression over weeks also helps to

identify the ulcers in which the healing trajectory is not normal. Once diagnosed and managed properly, the VLUs can heal in 24 weeks in 75-81% of the cases (Coyer, Edwards & Finlayson 2005). If the ulcers follow normal healing trajectory, there should be a reduction in the ulcer area by 50% in the first four weeks (Cardinal et al. 2008). However, the rates of healing in arterial and venous leg ulcers are not very well studied and have limited reported outcomes (Kranke et al. 2012).

(a)

(b)

(c)

(d)

Figure 2.5: An example of four weeks of a venous leg ulcer (images taken from dataset collected for this study)

2.4 Current assessment techniques

- **Area measurement using ruler technique**- This technique measures the area of the ulcer based on the assumption that it is approximately rectangular. The area of the ulcer is measured after the ulcer has received adequate debridement and slough/exudate has been removed. The maximum length and width is measured using a ruler, as shown in figure 2.6 and the product of these two measurements gives the area of the ulcer (Mani, Romanelli & Shukla 2012).

Figure 2.6: The measurement of area of an ulcer using ruler method (image taken from dataset collected for this study)

- **Area measurement using wound tracing**- Commonly, there are two types of wound tracing methods which are used in clinical settings- the manual planimetry (acetate) and the digital planimetry (Visitrak) (Gethin & Cowman 2006; Mani, Romanelli & Shukla 2012). The manual planimetry technique traces the area of the ulcer by placing a transparent sheet across the surface of the ulcer and tracing the margins with indelible ink. This tracing is then placed over a grid and the number of squares inside the circumscribed area are counted (Gethin & Cowman 2006; Khoo & Jansen 2016).

  The digital planimetry (Visitrak) involves contact tracing of the ulcer on a 2-layered transparent film and retracing the outline from the top layer film on a digital pad using the Visitrak pen, wherein the software calculates the area of the ulcer, as shown in figure 2.7 (Chang, Dearman & Greenwood 2011; Khoo & Jansen 2016). Visitrak also facilitates measurement of depth as it has depth gauge to measure cavity ulcers. Both these methods have the advantage of providing a permanent record for patient notes (Gethin & Cowman 2006; Barone, Paoli & Razionale 2011). Even though both tracing methods are easy to use and the area obtained using both methods is precise and

objective, the precision of digital planimetry is more reliable than ruler technique and manual planimetry (Khoo & Jansen 2016).

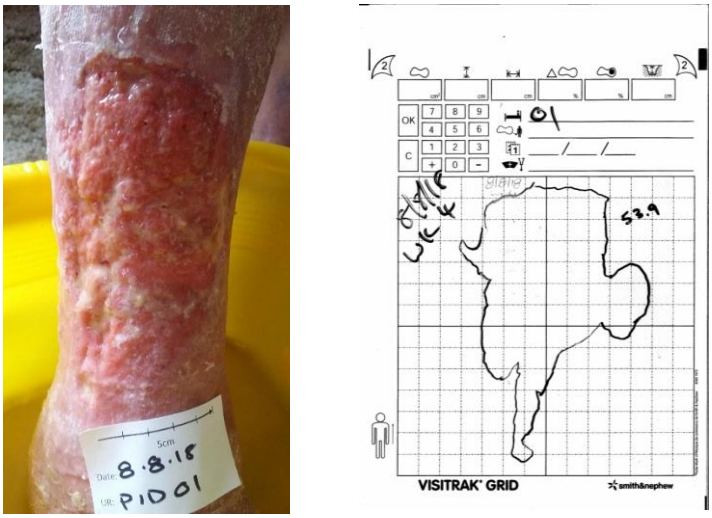

(a) (b)

Figure 2.7: The application of digital planimetry (Visitrak) on an ulcer (image and data taken from dataset collected for this study)

The more recent digital tracing is digital elliptical method (DEM) which uses techniques of optical photographic wound imaging and uses specific software to create a three-dimensional image of the ulcers. This image is fed into the computer to construct an accurate estimate of the size of the ulcer. However, this technique is not usually used in the clinical settings (Mani, Romanelli & Shukla 2012).

- **Irregularity analysis of the wound contours**- The wound edge plays an important role in the assessment of the ulcers. The examination of the wound edge to check whether it has gentle slope, well demarcated, punched out or rolled edges can provide key information about its aetiology and degree of malignancy (Grey, Enoch & Harding 2006). Even in the measurement of area of the ulcers, identification of the wound edge is an important criterion, to make accurate measurements (Gethin & Cowman 2006; Khoo & Jansen 2016). Literature has emphasized on change in the irregularity of the edge of chronic wounds as they heal, thus playing its role in wound healing as well (Menke et al. 2007). However, no quantitative study has been done yet to quantify the irregularity of the ulcer edges.
- **Thermal imaging of the ulcers**- Thermography has been used extensively for assessing the risk of developing ulcers on feet and for assessing the neuropathic and

ischemic conditions by measuring the change in foot temperature from normal (Mendes et al. 2015; Ring 2010). An infrared thermogram is obtained as the image to show temperature distribution of the feet. Each pixel in a thermogram has an intensity value equivalent to the temperature value, represented by a specific colour. The use of temperature distribution and monitoring has been used as a preventative and predictive tool for DFUs because there is a clear correlation between an increase in foot temperature and subsequent foot ulceration (Houghton, Bower & Chant 2013). Thus, thermal imaging has been used for early prediction of neuropathic ulcers (Kaabouch et al. 2010; Liu et al. 2015; Macdonald et al. 2016). Figure 2.8 shows an example of thermal image of an ulcer with its RGB image.

(a) (b)

Figure 2.8: (a) RGB image and (b) thermal image on a venous leg ulcer (images taken from dataset collected for this study)

- **Hyperspectral imaging of the ulcers**- Hyperspectral imaging records a cube of images of biological tissues over a narrow spectral band of wavelengths. The resulting set of images is a three-dimensional hypercube and consists of two spatial coordinates and one spectral coordinate (Vo-Dinh 2004). Thus, each pixel in a hypercube corresponds to the local reflectance spectrum of the tissue, represented by vectors corresponding to specific wavelengths and the size of the vector is equal to the number of spectral bands of the sensor. Figure 2.9 shows an example of a hyperspectral image of an ulcer with its RGB image. Hyperspectral imaging in the visible and near-infrared (NIR) parts of the spectrum has been applied in the monitoring of diabetic neuropathy and neuro-

ischemic conditions and prediction of the healing potential of DFUs by measuring the spatial distribution of oxygen saturation in biological tissues (Greenman et al. 2005; Nouvong et al. 2009; Yudovsky, Nouvong & Pilon 2010). It was found that the levels of oxyhemoglobin and total haemoglobin concentration increased first and then decreased over time in healing wounds and in cases of inflammation but remained constant in non-healing wounds (Khaodhiar et al. 2007; Martinez 2002; Stamatas & Kollias 2007; Yudovsky, Nouvong & Pilon 2010), while deoxyhemoglobin concentration remained relatively constant overtime in both healing and non-healing wounds.

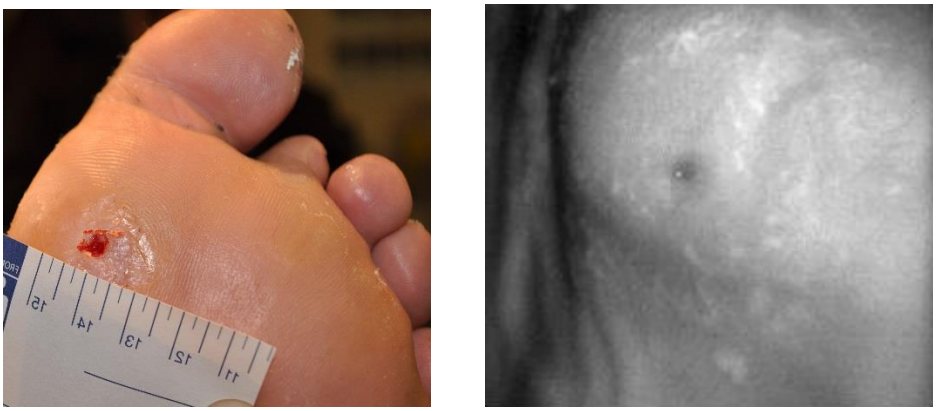

(a) (b)

Figure 2.9: (a) RGB image and (b) hyperspectral image of a diabetes-related foot ulcer (images taken from dataset collected for this study)

2.5 Limitations of the current assessment techniques

The conventional methods of ruler technique and manual planimetry are widely utilized in clinical settings for the assessment of ulcers because they are inexpensive and easily accessible. However, there are several limitations to these techniques. The ruler technique assumes the ulcers to be rectangular in shape. However, the ulcers are usually not in defined geometric shapes. Studies have shown that this method overestimates the area of the ulcers by 10-40%. Measurement of volume by this technique is also not reliable, as it lacks precision (Khoo & Jansen 2016).

Even though wound tracing (manual planimetry) is advantageous over the ruler method, it also has certain disadvantages. Since this technique involves direct contact with the surface of the ulcer, it has significant problems such as contamination of the wound bed, pain and discomfort to the patient and deformation of the wound size and shape (Khoo & Jansen 2016).

The measurement of area is a subjective measurement as there are variations in the skills and expertise of healthcare providers. Moreover, measurement of only area of the ulcers is not a reliable indicator of healing, as there are multiple factors playing role in the healing of these ulcers. Studies have shown that despite best management of the ulcers, 20% of them fail to heal within the given time frame of 12 weeks, even after showing early signs of healing within the first 4 weeks and require additional interventions to improve the healing process (Edwards, HE et al. 2018; Warriner, Snyder & Cardinal 2011). Figure 2.10 shows an example of a not-healed ulcer, which did not heal by week 12 even after showing early signs of healing. Delayed healing of the ulcers increases the risk of infection, followed by amputation of the lower limbs in the most severe cases. Also, much time is wasted before the clinicians identify that more aggressive intervention might be needed for the ulcers showing delayed healing, which increases the cost of care and the negative impact on HRQL of the patients. It has been reported in literature that healing of these chronic ulcers is a complicated multi-factorial process (Savage 2012; Yazdanpanah, Nasiri & Adarvishi 2015) hence they should not be assessed only by a single parameter, but multiple subjective and objective measurements should be taken.

(a) Week 1 (b) Week 2

(c) Week 3 (d) Week 4

Figure 2.10: An example of four weeks of a ‘not-healed ulcer’ showing 50% reduction in its area by week 4 but failed to heal by week 12 (images taken from dataset collected for this study)

Recurrence of ulcers is another problem which the clinicians must deal with. Around two-thirds of the ulcers are declared healed after treatment which can be a slow process, often taking more than a year. Thereafter, over half of them get recurrent ulceration within 12 months (Yazdanpanah, Nasiri & Adarvishi 2015). Hence there is a need for alternate objective assessment techniques for the ulcers, apart from measurement of area of the open ulcers.

2.6 Summary

This chapter has described two kinds of chronic ulcers in detail- diabetes-related foot ulcers and venous leg ulcers. The statistics on the number of individuals suffering from these ulcers has been discussed to emphasize on the need of attention on the assessment of the ulcers, as they have been widely ignored in Australia and other developed countries. The economic impact on healthcare and patients, and the impact on the health-related quality of life of the patients due to ulcers have also been discussed. The types of DFUs, the etiological factors associated with them and the interventions practiced by the clinicians has been explained. Similarly, VLUs and the etiological factors associated with VLUs along with the clinical interventions have also been explained. A brief review on the current assessment techniques of the ulcers has also been covered in this chapter, along with their strengths and limitations.

Based on the analysis of the works reported in literature and limitations reported above in section 2.4 and 2.5, this research study proposes the following:

- Development of two algorithms to quantify the irregularity in closed curves and boundaries of ulcers and to test the association of irregularity of ulcer contours with clinical conditions and healed status of ulcers.
- Use of thermal imaging to study the association of temperature with clinical conditions.
- Use of thermal imaging for differentiating between healed and not-healed ulcers based on the area obtained on the temperature distribution.

This thesis identifies the methodology to quantify the irregularity in 2D closed curves by the application of wavelet transform of their 1D profile (*chapter 3*), introduces a curve irregularity index to quantify the irregularity in 2D closed curves and shows its application on the contours of DFUs to test the association of irregularity with clinical conditions and to differentiate between healed and not-healed VLUs based on the irregularity in their edges (*chapter 4*). It studies the association of mean temperature of the ulcers with the clinical conditions as important factors affecting the healing of the ulcers (*chapter 5*). This work also investigates to

differentiate between the healed and not-healed VLUs based on the area obtained from the temperature distribution of the ulcers from their thermal images (*chapter 6).* Last but not the least, the thesis concludes by reporting the main contributions of the work and future studies (*chapter 7*).

Chapter 3

Quantification of irregularity of 2D curves using wavelet decomposition

3.1 Introduction

Roughness is an important property of natural objects and its quantification is required for any machine-based analysis. The most common method of quantification is by using Fractal Dimension, but most natural and biological objects are fractal only in a limited range. Furthermore, digitization introduces limited self-similarity and reduces the fractal properties of the objects; hence limits the use of fractal dimension for such applications. This research work has proposed a novel method to quantify the roughness/ irregularity in irregular curves and has tested it on synthetically generated curves. The advantage of this method is that it does not require the objects to have fractal properties for quantification of their roughness.

In this chapter, *section 3.2* highlights the importance of quantification of irregularity in irregular curves, gives a description on fractal dimension and addresses the limitations of fractal dimension to quantify roughness in natural and biological curves which do not show fractal properties. It also gives a review on the use of wavelet transform to quantify roughness in surface analysis. *Section 3.3* describes the method for generation of six sets of synthetic curves for validation of the method. *Section 3.4* describes the method for quantification of irregularity in the curve. The 2D curve is transformed to its 1D profile and discrete wavelet decomposition is performed on it. The RMS of the detail coefficients so obtained is computed and tested to obtain the detail coefficient corresponding to the irregularity of the curve. The investigated method is validated on synthetic curves of varying degrees of irregularity, which is described in s*ection 3.5*. Finally, *section 3.6* summarizes the main outcomes, advantages and limitations of the proposed method.

3.2 Irregularity analysis in irregular objects

Several curves in nature have irregular shapes and complex structures and cannot be quantified and described exactly by conventional Euclidean geometry (Shelberg, Moellering & Lam 1982). Euclidean measurements are suitable for approximating these curves for several other

applications such as measuring the area or volume. However, there are several applications where the irregularity or complexity of these curves are considered relevant and conventional geometric measurements are unsuitable in such cases.

Many natural and biological curves show fractal properties, and these properties can vary in their nature, appearance and origin. Sometimes, it is the geometrical shape of the boundaries (or contours) of the structures which show fractal properties, while other times, the fractal properties are somehow hidden, and can only be quantified by studying the data as a function of time, or by mapping it onto a graph (Havlin et al. 1995). The most common method of measuring the complexity of these structures is by Fractal Dimension (FD). Fractal objects exhibit specific properties, such as high level of organization, shape irregularity, scale invariance, iterative pathways, and functional, morphological and temporal self-similarity (show similar patterns at increasingly small scales) (Losa 2011).

FD has been an effective measure in description and characterization of the complexity in biological tissues which show self-similar properties (Carbonetto & Lew 2010; Jayalalitha & Uthayakumar 2007). The irregularity of the boundaries of biological objects possesses important information, which helps in the identification of the diseased conditions such as breast tumours and skin cancer. For the detection of malignant melanoma, Jayalalitha and Uthaykumar computed FD of the affected cells to detect the stages of the skin cancer using Box counting method and Sausage method (Jayalalitha & Uthayakumar 2007). The important diagnostic indicators such as complexity of the contours, colour and diameter of the cells were considered for classification. The complexity of the contours differs in normal moles (nevi) and melanomas, where melanomas are characterized by higher degree of complexity/ irregularity in their boundaries. To quantify the complexity, FD of the boundaries of normal moles and melanoma were computed using box counting method, used as the feature and a linear decoder was trained to perform the classification of the melanomas from normal moles (Carbonetto & Lew 2010). In another work, the range in which the skin lesions show fractal properties was identified using a modified approach of box-counting method, emphasizing on the multifractal properties of the lesion boundaries (Piantanelli et al. 2005). Multifractal analysis was also done to quantify complexity in the shape of epithelial-connective tissue interface (ECTI) in oral lesions (Landini & Rippin 1996).

FD has been shown to be very effective in measuring the irregularity in the above curves. However, unlike mathematical curves, which have the same fractal properties at all scales, the

fractal properties of biological objects can be observed only in a limited range or scale, referred to as "scaling window". The scaling window is experimentally established by considering the linear range of the log-log plot (of the number of self-similar pieces to the magnification factor) and keeping the scaling range for at least two orders of magnitude (Losa 2011). Therefore, these objects are known as semi-fractal or multi-fractal objects, as mentioned in the previous paragraph. Even the natural objects or curves are said to exhibit self-similar properties to only three or four levels of recursion (Cutting & Garvin 1987). There is another limitation arising due to the discretization of these objects. When these biological objects are captured as 2D digital images, the self-similar property is eliminated due to the inherent limited resolution of the digitized images, which makes these objects non-fractal. This limits the use of FD to quantify the irregularity in these objects.

The other concern is estimating FD requires linear regression which is meaningful only when there are enough points. The general rule of thumb is that 20 points provide evidence for linear relation in the log-log plot so obtained. There should also be at least two or three orders of magnitude to estimate self-similarity from the plot (Gonzato, Mulargia & Marzocchi 1998; Górski & Skrzat 2006). Only after considering the above two points, the data can be tested for linearity. If any of the conditions do not hold true, the value of obtained FD is not correct, and should not be considered as representative of the self-similarity of the data. The real problem in fractal analysis is the lack of sufficient data points. This makes it difficult to discriminate the self-similar objects from the cases where there is no self-similarity at all (Gonzato, Mulargia & Marzocchi 1998). Thus, having less data points would give incorrect or meaningless results and lead to wrong conclusions.

Another method for roughness analysis is wavelet transform-based methods as they have been successfully applied for surface analysis (Alhasan, White & De Brabanter 2016; Josso, Burton & Lalor 2002; Wei, Fwa & Zhe 2002). The main advantage of wavelet transform is its ability to provide multi-scale view of the frequency components of the signals at different decomposition levels (Chen, X, Raja & Simanapalli 1995). This advantage of wavelet decomposition has been used in this research work to develop a novel method to quantify the irregularity of curves which do not show self-similar properties.

3.3 Generation of synthetic images for validation

The proposed algorithm first transforms the 2D curve to its 1D profile, performs wavelet decomposition of up to five levels on it, computes the Root Mean Square (RMS) of the five

detail coefficients and selects the measure of irregularity from the RMS of five detail coefficients, based on which coefficient best differentiates the curves of different irregularity levels. The algorithm has been discussed in detail in section 3.5.

For validation of the algorithm, random irregular curves were synthetically generated. The irregularity in these curves was controlled by two parameters- by contracting and expanding the smooth curve along the radial (represented by equation 3.1), and by adding different magnitudes of noise to the generated curves (represented by equation 3.2). The smooth curve was first generated- *M* radials were drawn through the centre at equal angles and *M* points of intersection were located on the curve for each of the radials. The distance of these points from the centre was changed such that it was randomly generated to lie in the range r_{min} and r_{max}, computed from the defined centre, and described by equation (3.1). The r_{min} and r_{max} values were kept constant at 1.5 and 9 units respectively.

$$V_M = r_{min} + (r_{max} - r_{min}) * 0.1 * rand(M) \qquad (3.1)$$

The function *rand* in the above equation represents generation of *M* number of uniformly distributed random numbers between 0 and 1. For this work, *M* was kept constant at 20. The higher the value of *M,* the more irregular would be the curves.

Spline interpolation of these V_M points were performed to get the final curves; let I_{M_i} represent the interpolated values thus obtained, where M_i *=0,1,.....,M*. The interpolated values at the query points were based on cubic interpolation; a third order polynomial was computed from the values of the two neighbouring points in the respective dimension. Since the minimum number of query points required to evaluate the interpolant using spline interpolation is 4, the number of query points was heuristically set to 5.

For this work, r_{min}, r_{max} and *M* were kept constant, and the irregularity in these curves, as defined in this work, was changed only by adding noise of magnitude *n* to the interpolated curve, I_{M_i} using the following formula:

$$R_{M_i} = I_{M_i} + (-n + 2 * n * rand(M_i)) \qquad (3.2)$$

The second component of equation (3.2) represents the noise component added to the interpolated curve I_{M_i} to get the final noisy contour. The variable M_i in the equation represents the total number of interpolated values obtained after interpolation and R_{M_i} represents the resultant curve with the additive noise. The variable *n* in the equation varied from 0 to 0.5 in

intervals of 0.1, to obtain six sets of curves with varying irregularity- it was set to 0.0 for smoothest curves and 0.5 for the most irregular curves. The value of *n* can go beyond 0.5 to increase the irregularity in the curves; however, the maximum value for this work was set to 0.5. Thus, six sets of 30 curves, each set corresponding to different level of irregularity were developed. Figure 3.1 shows the six sets of curves with varying values of *n*. It should be noted that the irregularity mentioned here could represent irregularity in any irregular object and is not restricted to ulcer contours alone.

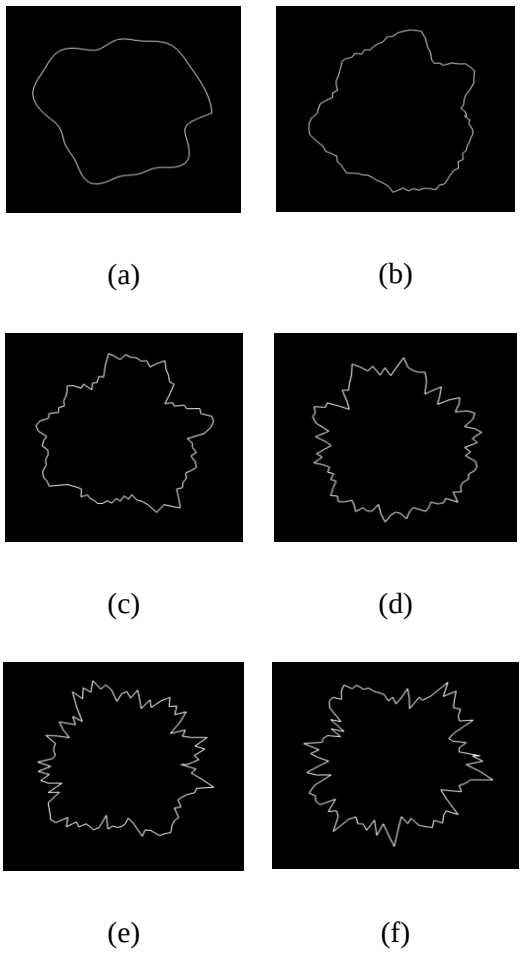

Figure 3.1: Examples of synthetic images with varying values of variable *n*, (a) *n*=0.0 (smoothest curve) (b)) *n*=0.1 (c) *n*=0.2 (d) *n*=0.3 (e) *n*=0.4 (f) *n*=0.5 (roughest curve)

3.4 Method for quantification of irregularity

The method consists of three main steps: i) transformation of the curve to 1D profile ii) wavelet decomposition up to five levels iii) computation of Root Mean Square (RMS) and selection of the measure of irregularity from the RMS of five detail coefficients.

3.4.1 Transformation of curves to 1D profile

The 2D curves' transformation to 1D profile for roughness analysis has been reported in literature (Pohlman et al. 1996; Rangayyan & Nguyen 2007). One of the methods derived the 1D of the contours of breast tumours to study their roughness by measuring the radial distance from the centroid of the contour to each contour point and plotting that as a function of the index of each contour point (Rangayyan & Nguyen 2007). The proposed method in this work has also followed a similar process. For this purpose, the first step required obtaining the centroid of the curve, which was obtained by fitting a minimum enclosing circle and then iteratively moving this to balance the centre of mass of the plane outlined by the curve. The centroid as the reference point makes the transformation invariant to rotation and translation (Raguso et al. 2010; Rahmati, Adler & Hamarneh 2012; Rangayyan & Nguyen 2007). The curve was converted into a 1D array by measuring the Euclidean distance between the centroid and each pixel on the curve, as shown in figure 3.2.

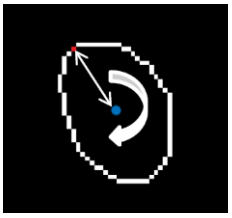

Figure 3.2: An example of a curve and its centroid (marked in the centre), with the starting pixel chosen as the one with maximum distance between the centroid and the pixel; the clockwise direction of tracking of pixels has also been shown.

Converting the curve into a 1D array requires the selection of an initial point. For repeatability, a rule was made, where the pixel which lies at the maximum distance from the centroid was considered as the starting point, x=0. Thus, the Euclidean distance between this pixel and the centroid was the value of the array at point x=0. A pixel-by-pixel continuous tracing of the curve was performed for 360^o and thus all the points of the curve were covered. Figure 3.3 shows two examples of the obtained 1D profile from the respective 2D curves. Smooth curves have smooth or circular contours; hence their resultant 1D profile is also smoother compared to irregular curves with rough contours, as can be seen in figure 3.3.

There might be some cases wherein two or more pixels would have the same maximum distance from the centroid. To overcome this limitation, a reference pixel should be chosen as the pixel which lies at zero degrees to the centroid in the horizontal axis. Out of the two (or more) pixels with the maximum distance, the pixel which lies at the minimum angle from this

reference pixel (in the clockwise direction) should be considered as the starting point. However, there were no such cases encountered in the images considered in this work, hence this rule was not used.

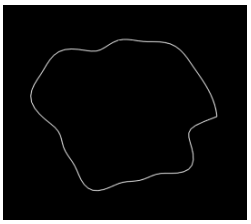

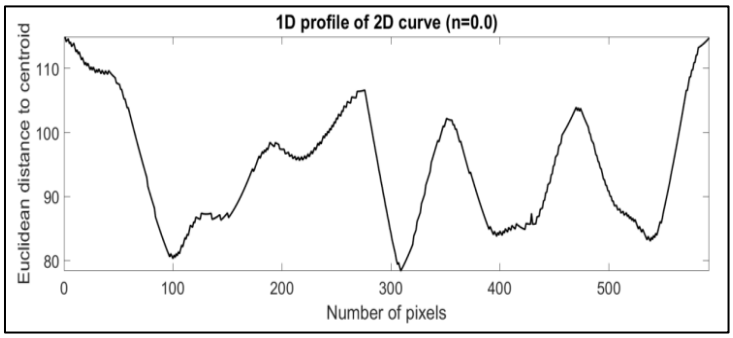

(a)

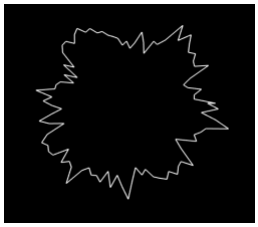

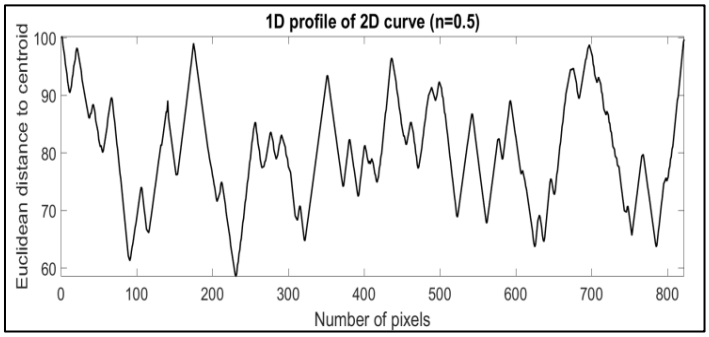

(b)

Figure 3.3: The 1D profiles (right) of the 2D binary curves (left) respectively

3.4.2 Wavelet decomposition of 1D profile

In this work, the irregularity of the curves has been defined based on the frequency content of their respective 1D profile and on the linear change of irregularity measure with change in irregularity of the curves. Thus, to extract the different frequency components from the 1D profile, discrete wavelet decomposition of up to five levels was performed on the 1D profiles using Daubechies 2 wavelet.

3.4.3 Computation of Root Mean Square (RMS) and selection of the irregularity measure

The Root Mean Square (RMS) values were computed for all the five detail coefficients and the RMS values were observed in the form of interval plots to identify the detail coefficient which

contains the frequency component corresponding to the irregularity of the curves. Figure 3.4 shows the interval plots of the five detail coefficients (d1, d2, d3, d4 and d5).

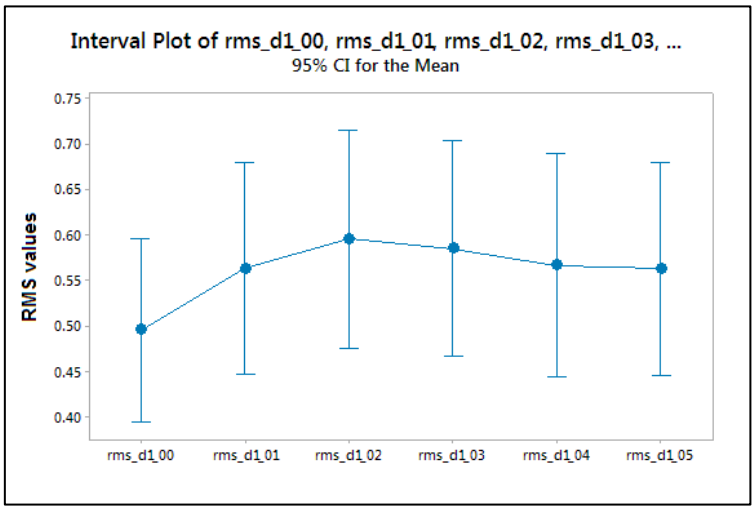

(a)

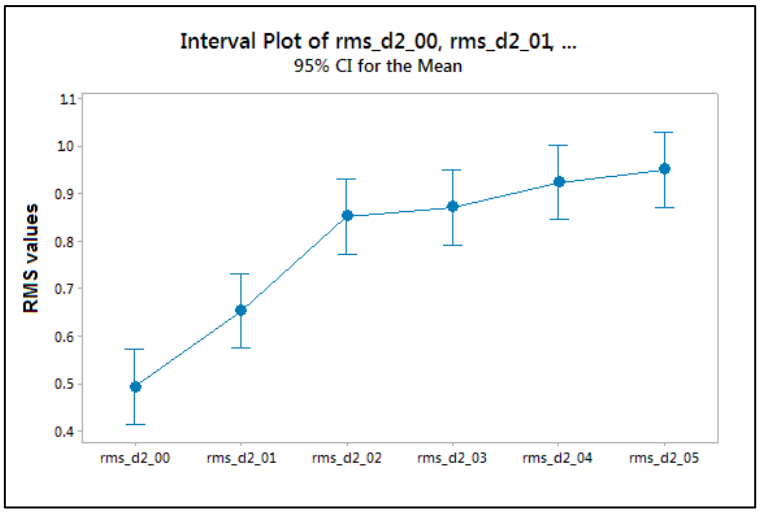

(b)

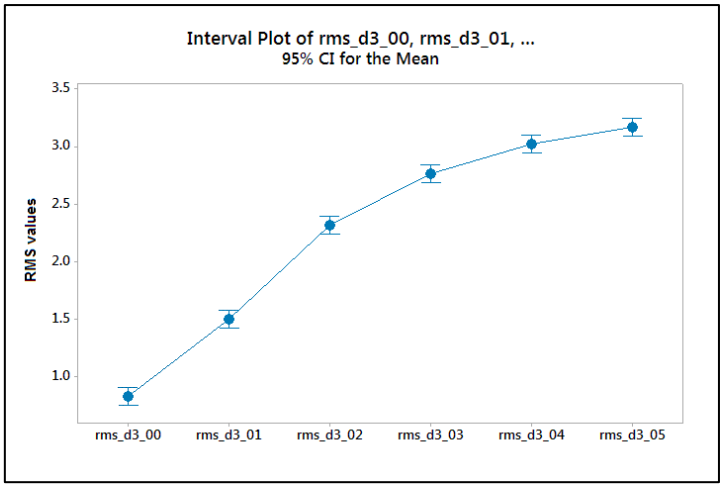

(c)

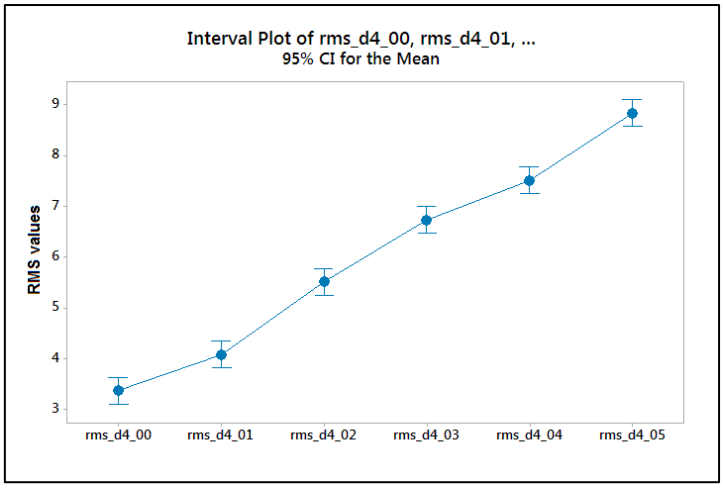

(d)

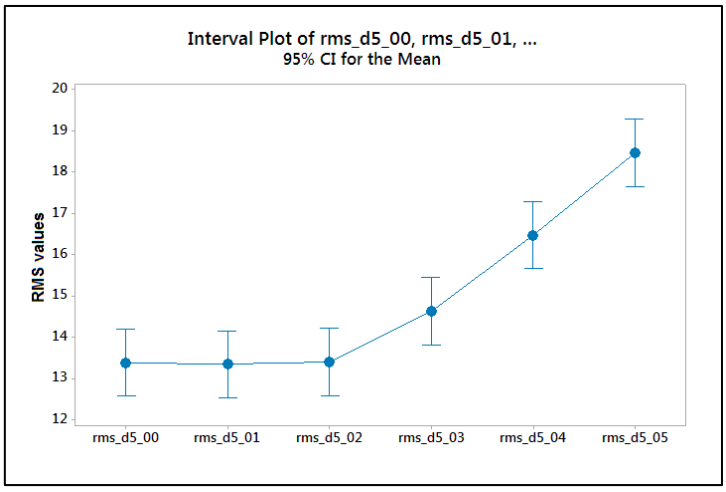

(e)

Figure 3.4: The interval plots of RMS of the five detail coefficients: (a) RMS (d1) (b) RMS (d2) (c) RMS (d3) (d) RMS (d4) (e) RMS (d5) for all groups of varying irregularity (n=0.0 through n=0.5)

From figure 3.4, it can be seen that the RMS of first detail coefficient (d1) did not give any information and could be attributed to digitization noise. The second detail coefficient (d2) could differentiate between the first two groups of curves, but showed knee point at n=0.2, hence could not differentiate between the other groups with higher degrees of irregularity. The third and fourth detail coefficients (d3 and d4) showed clear differentiation among the six groups of varying irregularity, hence the frequency corresponding to the irregularity of the curves was considered to lie in these detail coefficients, as the RMS values were distinct and unique to the individual groups of irregularity. Regression lines were fit on the mean of RMS values of d3 and d4, and a quadratic fit on d3 with R^2=0.99 and a linear fit on d4 with R^2=0.99 were obtained. The interval plot of RMS(d5) showed that the detail coefficient could differentiate the curves with higher degrees of irregularity but not the smoother ones, or the ones with low n values.

As mentioned before, the irregularity of the curves has been defined based on the linear change of irregularity measure with change in irregularity of the curves. Also, the change in irregularity of the curves has been introduced by linearly adding the noise magnitude n to the interpolated curves. Thus, even though the R-squared values are equally high for both d3 and d4, RMS of the fourth detail coefficient (RMS(d4)) has been considered as the measure of irregularity, as the mean RMS(d4) of the curves shows a linear change in irregularity with the change in noise, unlike RMS(d3).

3.4.4 Comparison with existing method

For comparison with this approach, the FD values were also computed for these 2D binary curves to show the sensitivity of FD for the change in irregularity. FD was computed using box-dimension method for binary data. Figure 3.5 shows the log-log plot of one of the smoothest curves (n=0.0) as an example and the FD value so obtained was 1.38, with minimum error for the linear fit. If all 20 points shown in the plot were to be considered (as reported in literature), the FD value would be 0.59 and with a large error value of 29% as the plot would not be considering the linear range alone. Hence the maximum number of points considered on the log-log plot was 8 for all the reported values, which means the scaling range of about two orders of magnitude was considered for the measurement. Figure 3.6 shows the interval plots of FD values for varying degrees of n. It can be seen from the interval plot that FD does not show any trend and hence fails to give us any information about the irregularity of the curves.

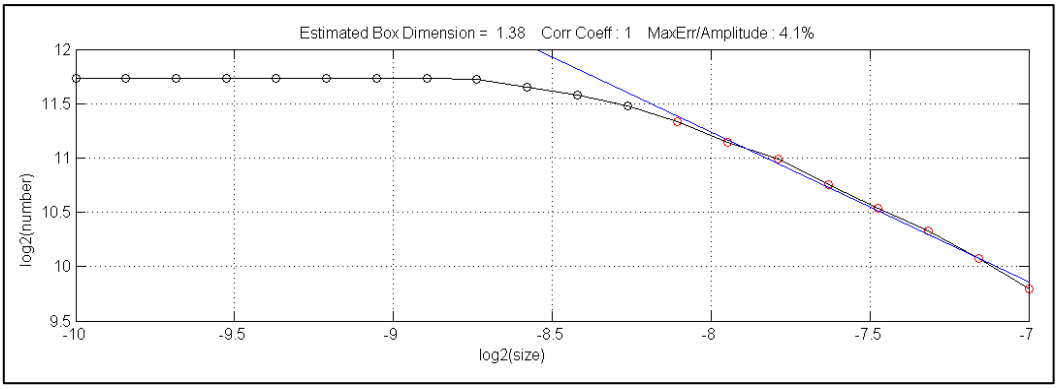

Figure 3.5: The log-log plot for FD calculation of one of the synthetic curves as an example

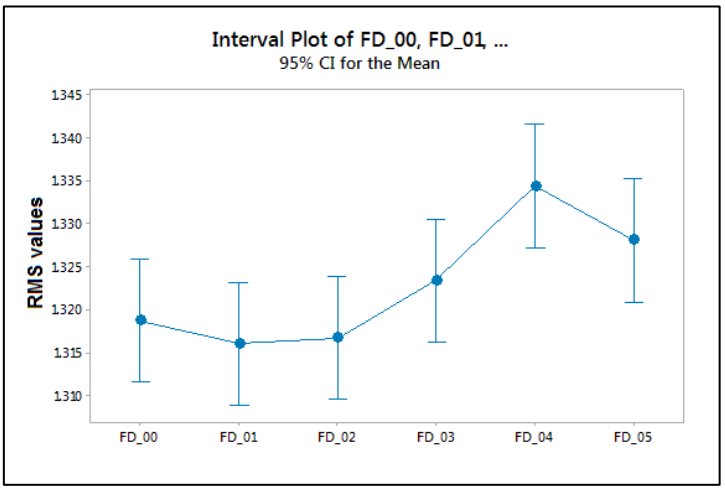

Figure 3.6: The interval plot of FD values of smooth curves, *n*=0.0 (FD_00) with increasing irregularity in the curves (FD_00 through FD_05)

3.5 Validation of the method

To test the hypothesis of whether this irregularity measure can differentiate among the curves having different levels of irregularity, the RMS(d4) values of the curves were tested for normality using the Anderson-Darling test and were found to be normally distributed. One-way ANOVA was performed on RMS(d4) to test the statistical significance among the groups of varying irregularity. Table 3.1 shows the results of ANOVA, considering 95% confidence interval (C.I.) of the mean.

Table 3.1: ANOVA results for RMS(d4) using the investigated method considering 95% C.I. for the mean

n (noise magnitude)	***p*-values for normality**	**Mean**	**95% CI**	***p*-value**
0.0	0.59	3.36	(3.10, 3.62)	<0.001
0.1	0.57	4.07	(3.81, 4.33)	
0.2	0.67	5.51	(5.25, 5.77)	
0.3	0.40	6.73	(6.47, 6.99)	
0.4	0.61	7.50	(7.24, 7.77)	
0.5	0.45	8.83	(8.57, 9.09)	

3.6 Summary

This chapter proposed a simple yet novel method for quantification of irregularity without assuming the curves to be fractal, and validated it using a set of synthetically generated images, thus overcoming the limitation of digitization and image resolution. The 2D curves were first transformed to their 1D profile and wavelet decomposition was performed on them. It was found that the mean RMS of the fourth detail coefficients had a linear relationship with the added noise to the shape of the curves- noise indicating the irregularity of the curves. The third and fourth detail coefficients of the curves (d3 and d4) showed clear differentiation among all the six groups. While d3 showed a quadratic trend in the mean RMS values, d4 showed a linear trend with increasing *n*, which was in agreement with the definition of irregularity considered in this research work.

The main advantage of the proposed method is that it works on curves without requiring the curves to display fractal properties (figure 3.4). Further, the interval plot of FD values (figure 3.6) for the same curves shows that computed FD does not have a linear or even monotonic relationship with the noise (or irregularity). Since the method works without assuming the fractal nature of the curves, it can be applied in assessing the contours of biological objects where the irregularity or roughness is often used for diagnosis, such as classifying skin melanoma from normal moles. This method can also find applications on other abnormalities, such as skin lesions and all types of wounds/ ulcers.

Despite this method being simple and novel, the possible limitation comes if the frequency (or irregularity) of the curves is increased further beyond the range considered in this work. There is a possibility that the measure of irregularity would shift to a higher detail coefficient than fourth detail coefficient (d4), showing knee points at d4 for higher degrees of irregularity, as

can be seen in the case of RMS(d2) in figure 3.4(b). Due to the above limitation, the method has not been implemented on ulcer contours. Hence another novel method has been proposed in the next chapter which overcomes this limitation and is more sensitive to the irregularity of the curves.

Chapter 4

Curve irregularity index for quantification of irregularity in irregular curves- development and validation

4.1 Introduction

As mentioned in the previous chapter, fractal geometry is widely used to study the roughness of irregular curves and this has several biomedical and geological applications. However, many natural and biological objects are semi-fractal, multi-fractal or non-fractal objects, where the fractal dimension (FD) measure does not work.

In this research work, a curve irregularity index (I_c) has been proposed to measure the irregularity of the curves (or shape of objects), which does not assume the curves to have self-similar properties. A comparison has also been done between this proposed index with FD using a set of synthetically generated curves having progressively increasing irregularity. The index has also been implemented on DFU and VLU datasets to test the association of contour irregularity with clinical conditions and the healed status respectively.

In this chapter, *section 4.2* highlights the importance of quantification of irregularity in irregular curves, gives a description on fractal dimension and addresses the limitations of fractal dimension to quantify roughness in natural and biological curves which do not show fractal properties. *Section 4.3* describes the role of irregularity of ulcer contours in the assessment of the healing status of DFUs and VLUs and the need of a novel method to quantify it. *Section 4.4* describes the three datasets generated for validation of the proposed method-generation of six sets of synthetic curves with varying degrees of irregularity, segmentation and binarization of DFU and VLU images to get binary contours. *Section 4.5* describes the method for quantification of irregularity in the curves and to obtain the curve irregularity index (I_c). The investigated method is validated on synthetic curves of varying degrees of irregularity and on ulcer contours, which is described in s*ection 4.6*. Finally, *section 4.7* summarizes the main outcomes, advantages and prospective of the proposed method.

4.2 Irregularity analysis in irregular objects

Many irregular natural and biological objects and events show self-similarity (Havlin et al. 1995) wherein Euclidean geometry becomes unsuitable for measuring their irregularity (Shelberg, Moellering & Lam 1982). Objects that display self-similarity are referred to as fractal objects and these exhibit properties such as high-level of organization, shape irregularity, scale invariance, iterative pathways and functional, morphological and temporal self-similarity (Losa 2011). Fractal dimension (FD) is a quantification of the fractal properties and is a measure of the self-similarity of the curves.

Studies have shown the association of the fractal geometry parameters of biological objects such as cells, tumours, skin lesions and vasculature with associated diseases (Guo et al. 2005; Kikuchi et al. 2002; Landini & Rippin 1996; Lee, McLean & Atkins 2003; Mu, Nandi & Rangayyan 2008; Rangayyan & Nguyen 2007). The irregularity analysis using FD has been found useful for diagnostic purposes, such as to distinguish between benign and malignant tumours and skin lesions (Landini & Rippin 1996; Lee, McLean & Atkins 2003). More literature on this topic has been covered in section 3.2.

The limitations of FD in the study on biological tissues has also been reported in section 3.2. Hence, many biomedical image analysis studies reported in literature lack the rigor of analysis; the assumptions on the use of FD have not been clearly stated and thus the interpretation of the results might be flawed. Thus, there is a need for an alternate method to quantify the irregularity of the shape of objects without assuming them to be fractal.

One of the common methods of measuring fractal dimension is the box-counting method. In this method, the object is covered with small cells (or boxes) of definite size and the number of boxes covering the object is noted. The above procedure is repeated by increasing the size of the boxes, and FD is determined by considering the slope of the log-log plot of the number of boxes covering the object by the size of the boxes. The basic theory of this method has been used to develop a novel method in this research work to measure the irregularity of the objects which fail to show fractal properties. The proposed method measures the change in irregularity with the change in scale by considering small sections of the curve and integrates all the irregularity values over different scales to obtain the final irregularity measure.

4.3 Roughness analysis in ulcers

Currently, the only parameter considered for the assessment of ulcer is the area of the ulcer region and its reduction over the weeks. However, examination of the wound edge in terms of whether it has gentle slope, well demarcated, punched out or rolled edges can provide key information about its aetiology and degree of malignancy (Grey, Enoch & Harding 2006). Literature also emphasizes on the change in the complexity (or, roughness) of the ulcer as it heals, thus playing its role in the assessment of the healing status of the ulcers (Menke et al. 2007).

As FD has been employed for quantification of complexity in other biological tissues, it could be employed to characterize DFU and VLU contours as well. However, with the limitations of FD mentioned in the above section, use of FD is limited in this case. Therefore, a novel method has been proposed in this research work which overcomes this limitation.

4.4 Datasets for validation

4.4.1 Synthetic images

The synthetic images generated in chapter three for validation of the algorithm has been used in this chapter for validation as well. Please refer to section 3.3 for the details on generating the synthetic images of varying irregularity. Figure 4.1 shows the six sets of curves with varying values of *n*.

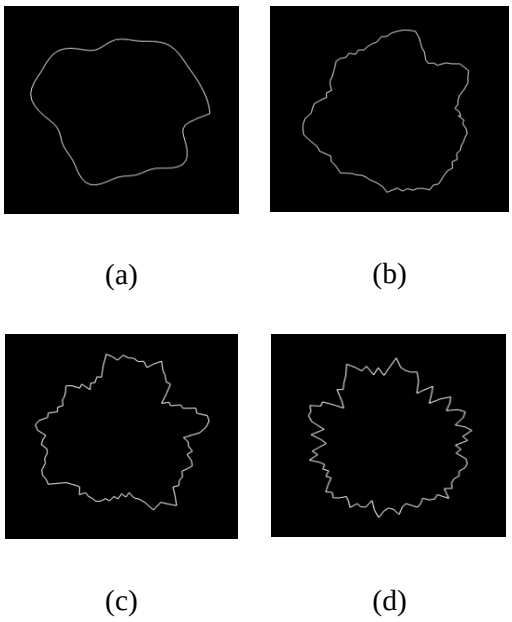

(a) (b)

(c) (d)

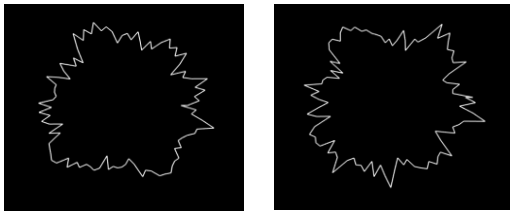

(e) (f)

Figure 4.1: Examples of synthetic images with varying values of variable *n*, (a) *n*=0.0 (smoothest curve) (b)) *n*=0.1 (c) *n*=0.2 (d) *n*=0.3 (e) *n*=0.4 (f) *n*=0.5 (roughest curve)

4.4.2 Diabetes-related foot ulcer images

Twenty-four inpatients and outpatients with type I and type II diabetes aged 30 and over who attended Austin Health, Melbourne, Australia for the management of DFUs, were recruited in this study as participants. All patients received standard medical care by the medical unit including ulcer debridement, dressings, offloading and dosage of antibiotics for ulcer infection. Some of the important information collected from the participants were: participants' demographics such as age, gender, past and current medical history, especially regarding their diagnosis and treatment of diabetes, the duration and description of the foot ulcer, associated clinical conditions such as Peripheral Vascular Disease (PVD), Ischemic Heart Disease (IHD) and Chronic Kidney Disorder (CKD) among others.

The data collection was performed by the Biosignals Lab at RMIT and was provided to me for image analysis. The images were taken by one trained person to keep the data collection consistent. The ulcers were photographed on a weekly basis using Nikon D90, digital DSLR camera in uncompressed RAW format (.NEF) over four consecutive weeks. Approval for this study was granted by the Human Research Ethics Committee (HREC) of the Royal Melbourne Institute of Technology (RMIT University), Melbourne, Australia as well as the HREC of Austin Health, University of Melbourne. All ulcers received proper debridement prior to photography to remove dead skin and to maximize the contrast between the wound edge and the wound bed. For each patient, the time of their admission in the hospital was considered as the baseline for the measurements. Only the green channel of RGB images were used for the analysis as they provided better contrast between the wound bed and wound edges. In this research work, images of only week 1 and week 4 were considered to measure the contour irregularities and the change in the irregularity from week 1 to week 4 was recorded and was used to test the association against the underlying clinical conditions of IHD, PVD and CKD.

4.4.2.1 Image registration

Although the images were captured by the same camera, they differed slightly in orientation and scales from each other. Therefore, image registration was performed to align the images which belonged to the same participant but had been captured in different weeks. To perform registration, green channel of the week 1 image was considered as the reference (source) and week 4 image of the same ulcer was considered as the target image. An automatic feature-based algorithm in MATLAB 2016a software (Image Registration toolbox) was used in this work, which aligned the images by selecting matching features between the two images shows an example of two registered images corresponding to week 1 and 4 of a participant. The image processing toolbox in MATLAB is an app which lets the users automate image processing techniques, including image registration. The app uses salient features of the images, in the cause of ulcer images, the registration was performed with respect to the toes and fingers in the images.

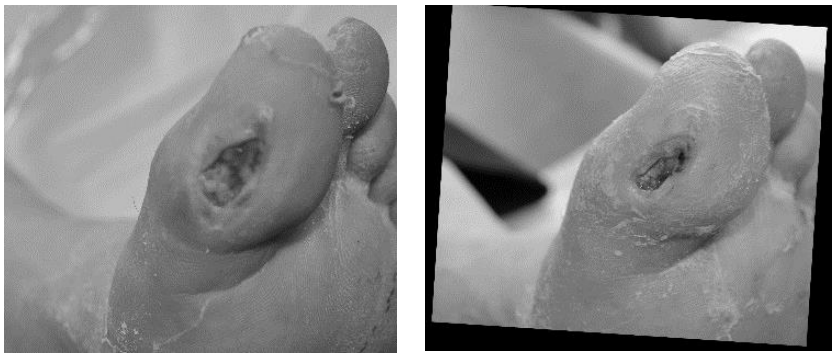

(a) (b)

Figure 4.2: Registration of the ulcer: (a) Ulcer image from week 1 (source image) (b) Registered ulcer image from week 4 (target image)

4.4.2.2 Segmentation of the DFU contours

Segmentation of the DFU contours was done using a bio-inspired active contour model, also known as Snake algorithm which has been reported very effective in literature for segmentation of skin lesions and ulcers (Hettiarachchi et al. 2013; Trabelsi et al. 2013). The snake-model is a "controlled continuity spline" which is controlled by the image forces and also guided by user defined external forces (Kass, Witkin & Terzopoulos 1988). Snake is an energy minimizing active model which exhibits dynamic behaviour. It is acted upon by two energy functions; internal energy of the spline ensures smoothness of the contour while the external energy represents the features of the ulcer and is provided by the user by defining initial points on the contour representing approximate location of the boundary (Kass, Witkin & Terzopoulos

1988). The algorithm takes the two energy functions and iterates until it locks into the local minimum positions and gives the final ulcer contour.

While there are different variants of snake models, including basic active contour, active gradient vector flow (GVF) B-spline and B-spline GVF, the latter was used in this work as it was shown to be suitable for delineating volume of interest with fewer required number of initial sample points compared to other models (Yang & Papa 2016). The fewer initial sample points reduces the manual work of the user of placing many points, especially in case of big contours. The open source MATLAB code of the algorithm was used, where the initial feature points were provided by me in all cases, to maintain consistency. The initial points were uniformly placed around the contour- the number of points being dependent on the size of the contour. Since the end result was sensitive to initial placement of points, the points were placed uniformly, but focusing more near the turning points of the contours and sharp edges of the contours, to guide the algorithm to give more accurate contour. The algorithm required the images to be in grayscale, hence the images were converted from RGB to grayscale for the application of the algorithm. Figure 4.3 shows an example of snake after the energy minimization algorithm pulled the snake to fit the ulcer contour, and the final binary contour obtained thereafter.

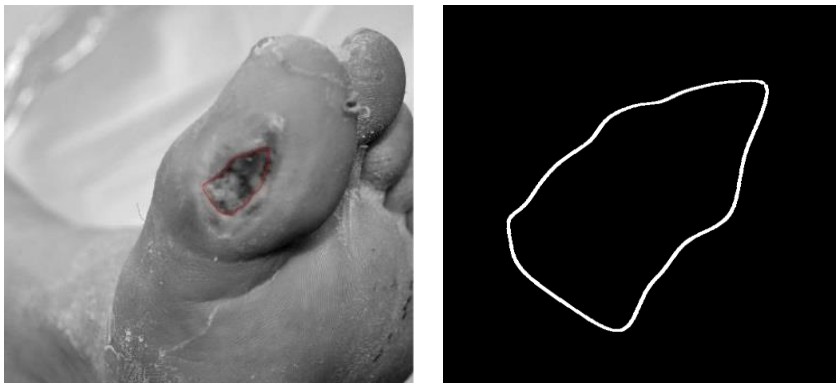

(a) (b)

Figure 4.3: Segmentation of ulcer contour using Active Contour Snakes model: (a) The snake fitted to the ulcer contour (b) Final segmented binary contour

4.4.3 Venous Leg Ulcers

All individuals aged 18 years or above with leg ulcers being attended by Bolton Clarke, Melbourne, Australia were recruited in this study. The inclusion criteria were presence of venous leg ulcers, with Ankle Brachial Pressure Index between 0.8-1.2 and having signs of venous diseases using clinical, aetiological, anatomical and pathological (CEAP) classification

system (Rabe & Pannier 2012). The ulcers from the ankle region to below the knee region were considered in this study. Out of the total of 80 participants enrolled in this study, only 36 participants who satisfied the above inclusion criteria were considered for this study, as the complete data of these participants were available at the time of this research.

The data collection was performed by the nursing staff of Bolton Clarke who attended the participants in their homes to provide care and treatment for the ulcers. The data management and image processing on the data was performed by me. Initial clinical assessment was done for all participants in the baseline week- demographic information, comorbidities information and wound related information were obtained. All the ulcers received standard wound care from the baseline week until the wounds healed. These ulcers were weekly attended by the nurse to provide care in terms of appropriate dressings and effective compression. The contours of the ulcers were obtained in each week using digital planimetry technique as standard clinical practice to assess the healing status of the ulcers. The RGB images were also collected to provide reference for the location of the ulcers. Figure 4.4 shows the RGB image of a VLU and its respective tracing of the contour. This study was approved by Human Research and Ethics Committee of Boston Clarke and RMIT University and written consents of the participants were also obtained in the baseline week for the study.

4.4.3.1 Morphological processing of the VLU contours

The VLU contours were obtained from the digital planimetry tracings of the ulcers. Since the tracings were obtained by placing the acetate paper in contact with the ulcer, there were no issues of variations in scale and rotation, hence registration was not required for the tracings. The tracings were converted to binary and morphological processing of erosion was performed to remove the grids and other unnecessary sketches from the images. Finally, the images were skeletonized to obtain single pixel thick contours for the algorithm to run smoothly.

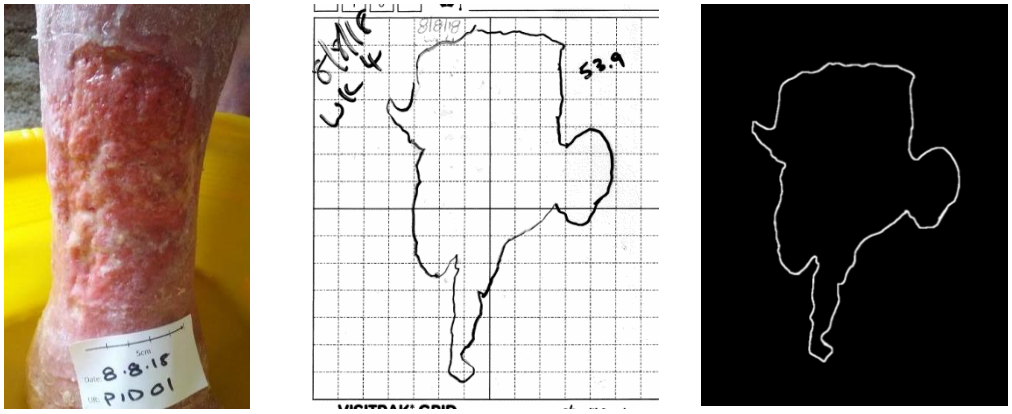

(a) (b) (c)

Figure 4.4: (a) RGB image of a VLU (b) Digital planimetry tracing of the VLU (c) Binary, skeletonized image of the ulcer contour

4.5 Measurement of curve irregularity index (I_c)

The new index measure proposed in this research work is called the curve irregularity index (I_c) and is defined as the integration of the mean of ratios of the shortest distance of the end-points of the curve segment to the length of the curve segment, with the curve segment window incrementing from 4 pixels to half of the total pixels on the curve, while sliding over the length of the curve. All the curves studied in this research work are closed binary curves with thickness of one pixel. The start of the calculation of the index is after random selection of the location of the first segment on the curve.

As the first step, window segment of length s is randomly located on the curve and local irregularity of that segment is calculated by the following formula:

$$I(s) = \frac{d(p_1,p_s)}{dP} \tag{4.3}$$

where $d(p_1,p_s)$ is the Euclidean distance between the end pixels p_1 and p_s, while dP is the total Euclidean distance of s consecutive pixels (p_1 to p_s) in the window segment s. The ratio $I(s)$ so obtained is the local irregularity for the segment length.

This process is repeated using moving and overlapping windows over the entire curve, shifting the curve one pixel at a time in the clockwise direction until the window moves over the entire curve and repeats the first segment again which ensures rotation invariance. Once the local irregularity values for a window length is calculated, mean of the $I(s)$ values are calculated for the respective window length. A pictorial representation for window size $s=10$ and $s=12$ is shown in figure 4.5.

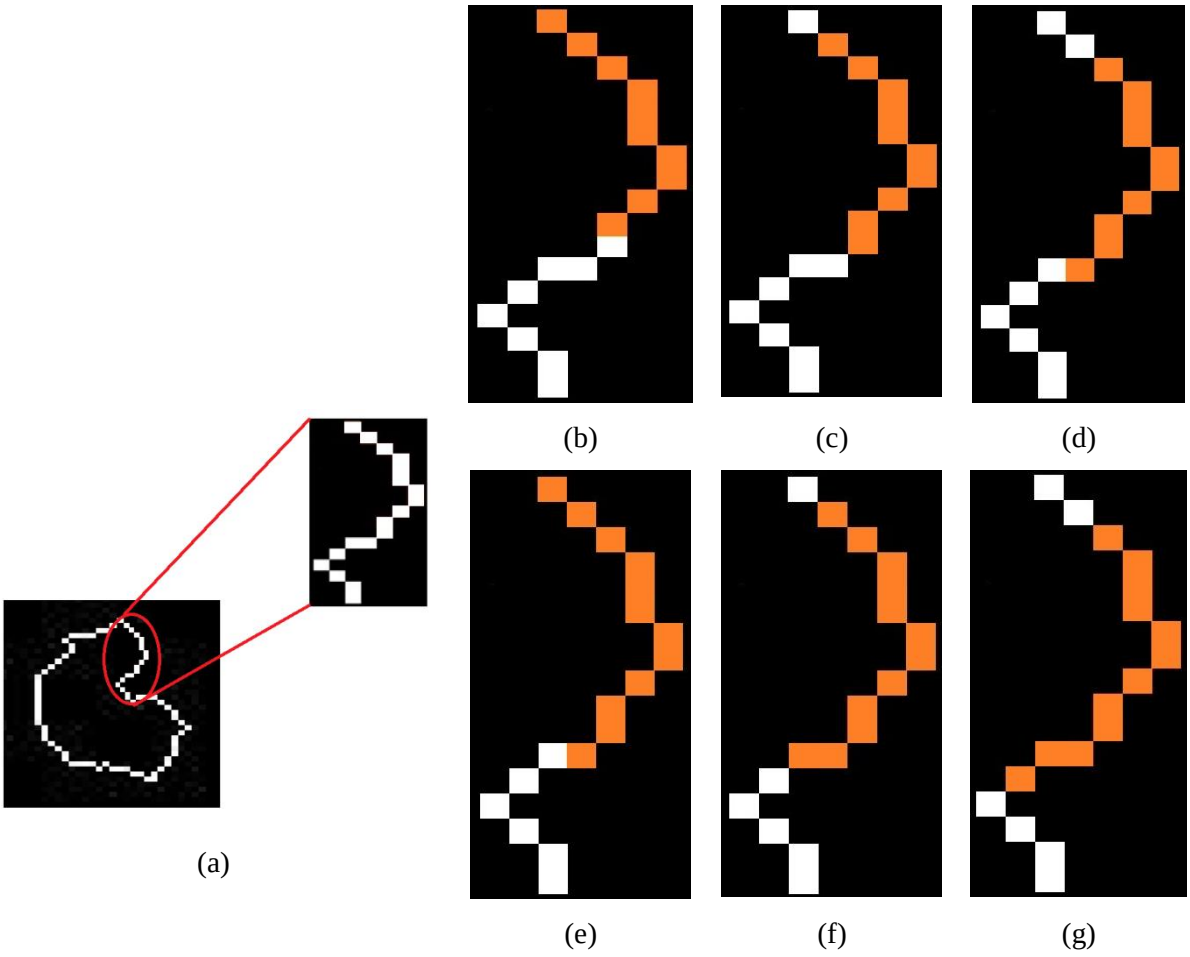

Figure 4.5: (a) example of a closed curve and a small segment of it, (b, c and d) example of *s=10* and its movement over the pixels, and (e, f and g) example of *s=12* and its movement over the pixels for calculation of irregularity

This iterative process is repeated with window segment lengths incrementing by 2, which was chosen because that was the smallest value to obtain significant change in *I(s)*. The smallest value for window segment of length *s* was taken as 4 because the ratio *I*(*s)* is equal to 1 for *s*= 1 or 2 and does not change significantly for *s*=3.

Considering the total number of pixels on the curve as *N*, the window length starts from 4 and goes up to *N/2* pixels, rounded up to the nearest whole number. The total number of window segment lengths for a closed curve of length *N* will be given by the formula,

$$t_s = \frac{N-8}{4} + 1 \qquad (4.4)$$

After computing the mean values of all window segment lengths, the curve irregularity (I_c') is obtained by performing discrete integration of *I(s)* using trapezoidal method.

$$I_c' = \int_{4}^{t_s} \sum_{\substack{4 \le j \le \frac{N}{2} \\ j \text{ is a multiple of } 2}} \frac{1}{N+1} \sum_{k=1}^{N+1} I(s)_{jk} \qquad (4.5)$$

where *j*= window segment lengths and *k*= segments on the curve of length *j*.

The irregularity feature of the curve is inversely proportional to the local irregularity, $I(s)$; higher the irregularity in the curves, smaller is the value of *I(s)*. However, this can be dependent on the size of the curve. Hence this was normalized using circle having the circumference equal to *N*, the total number of pixels of the curve. The normalization was performed by dividing the I_c' value of the curve by the I_c' value of its respective circle. This normalization made the values to be bound between 0 and 1, with the higher values indicating smooth curves, and lower values indicating irregular curves.

$$I_c = \frac{I_{c\,(curve)}'}{I_{c\,(circle)}'} \qquad (4.6)$$

The methodology has been illustrated in a block diagram below:

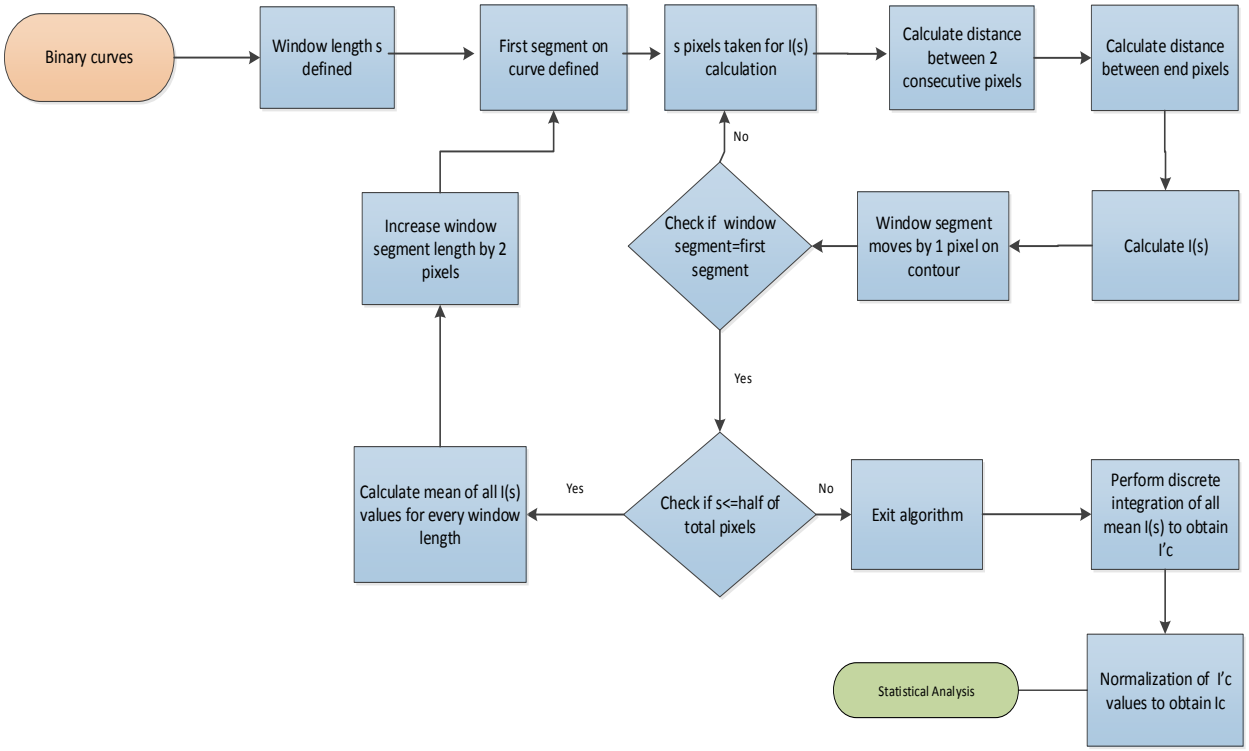

Figure 4.6: Schematic diagram showing the steps of the algorithm

4.6 Results

The objective of this research work was to validate the proposed method on:

(i) synthetic curves with varying levels of irregularity and to study the comparison of the proposed method with existing method (FD), and

(ii) contours of DFUs as examples of biological non-fractal curves- to quantify their contour irregularities and to study the association of contour irregularity with clinical conditions.

(iii) contours of VLUs as examples of biological non-fractal curves- to quantify their contour irregularities and to study the association of contour irregularity with the healed status of the ulcers.

4.6.1 Synthetic images

The irregularity index (I_c) and FD using box-counting approach were computed for each of the curves; box-counting approach was selected for FD based on its popularity in literature. The FD analysis of the data showed that the maximum number of points on the log-log plot was 8, indicating scaling range of about two orders of magnitude, which is less than the required 20

points (Gonzato, Mulargia & Marzocchi 1998; Górski & Skrzat 2006). While this indicates the unsuitability of using FD, however, for comparison, it was computed and used.

Figure 4.7 shows the interval plots of FD values and I_c values for varying degrees of n. It is observed that there is no observable trend using FD while there is a good linear, decreasing trend for I_c with a linear fit of R^2=0.99. Also, it should be noted from the figure that the I_c values are distinct for each value of n. This is further shown in the form of histograms. Figure 4.8 shows the histogram plots for I_c values of curves, showing the change in the range of I_c values with change in irregularity n. The distinct Gaussian peaks for each value of n confirm that the I_c values are distinct for each n.

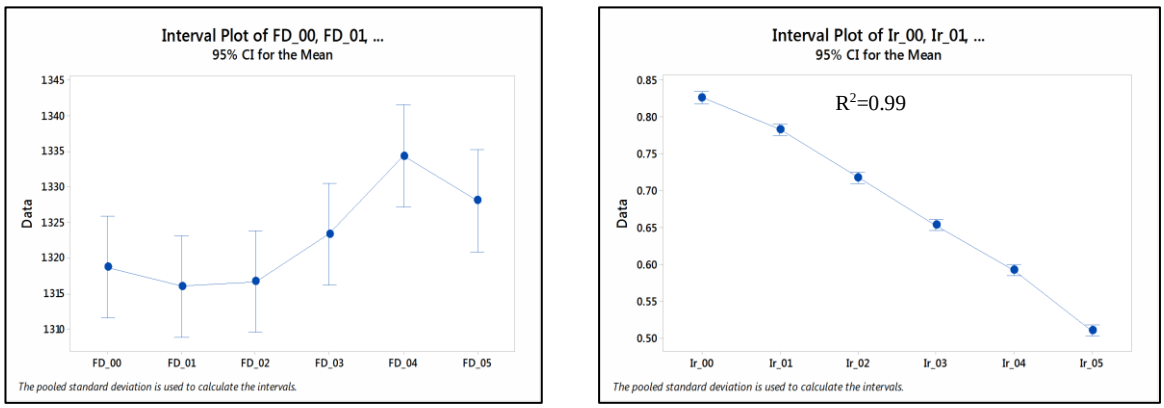

(a) (b)

Figure 4.7: The interval plots of (a) FD values of smooth curves, n=0.0 (FD_00) with increasing irregularity in the curves (FD_01 through FD_05) (b) I_c values of smooth curves, n=0.0 (I_r _00) with increasing irregularity in the curves (I_r_01 through I_r_05)

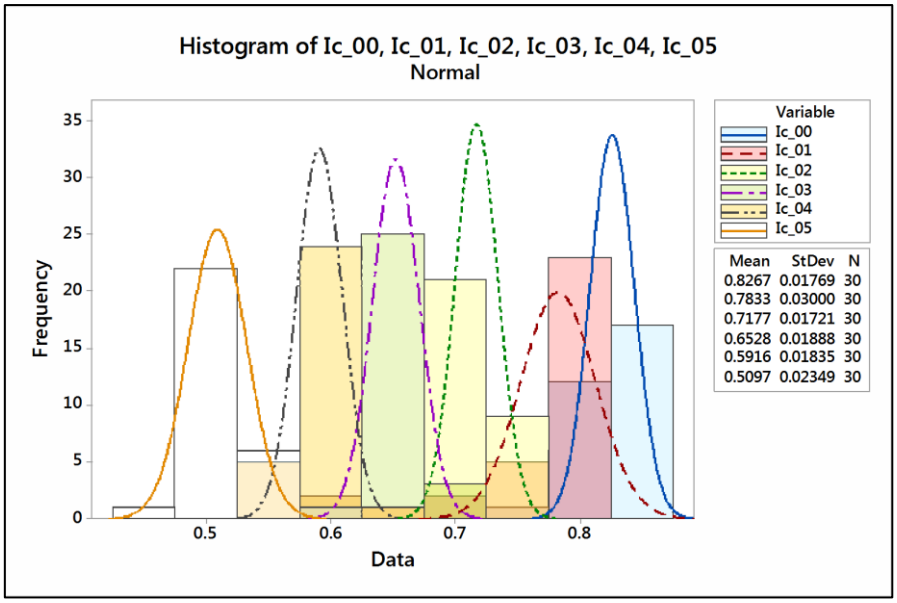

Figure 4.8: The histogram plots for I_c values of curves with decreasing roughness (towards right)

The data was tested for normal distribution and were found to be normally distributed (all *p-values*> 0.05) and subsequently, one-way ANOVA was performed using Fischer's exact method to investigate the significant difference among the values of the index for six levels of irregularity in synthetic curves. The ANOVA results in table 4.1 show that the proposed irregularity index showed significant difference among the six groups of curves having different irregularities (with *p-value*<0.001).

Table 4.1: ANOVA results for irregularity measurement of synthetic curves using the proposed method, considering 95% C.I. for the mean

n	***p*-values for normality**	**Mean**	**95% CI**	***p*-value**
0.0	0.59	0.83	(0.82, 0.83)	<0.001
0.1	0.57	0.78	(0.78, 0.79)	
0.2	0.67	0.72	(0.71, 0.72)	
0.3	0.40	0.65	(0.64, 0.66)	
0.4	0.61	0.59	(0.58, 0.59)	
0.5	0.45	0.51	(0.50, 0.52)	

4.6.2 DFU contours

To investigate significant association between contour irregularity and clinical conditions in DFUs, the I_c and FD values were computed for week 1 and week 4 ulcer images from 24

participants. The difference in I_c values of week 1 and week 4 and the difference in FD values of week 1 and week 4 were considered for statistical analysis. To test the hypothesis of whether the proposed method of irregularity holds any association with the clinical conditions under consideration (i.e. IHD, PVD and CKD), one-way ANOVA was performed using Fischer's exact method. The FD values were also tested to show association with the clinical conditions using the same statistical method. Out of the total of 24 participants considered for this study, the number of participants affected with IHD were 7, with PVD were 13 and with CKD were 12. The data was tested for normality prior to ANOVA analysis using the Anderson-Darling test, which gave a *p*-value of 0.455 for I_c and the *p*-value of 0.763 for FD, thus showing evidence that both parameters followed a normal distribution.

The results obtained from ANOVA have been tabulated in table 4.2, comparing the *p*-values obtained for the different clinical parameters, as well as the 95% C.I. for the mean difference between week 1 and 4. While the proposed measure of change in irregularity showed good association with IHD, the FD values showed no association with any of the clinical conditions. Figure 4.9 shows the interval plot of I_c with respect to IHD which shows that there is a significant difference between the means of the two data.

Table 4.2: ANOVA results showing p-values for irregularity and FD with the clinical conditions, considering 95% CI for the mean

Clinical parameters		**Irregularity***	**FD***
IHD	***p-value***	0.028	0.706
	95% CI	(-140.44, -9.09)	(-0.02, 0.02)
PVD	***p-value***	0.995	0.293
	95% CI	(-67.26, 66.89)	(-0.01, 0.03)
CKD	***p-value***	0.215	0.834
	95% CI	(-104.19, 24.79)	(-0.02, 0.02)

* The reported values correspond to the difference between week 1 and week 4 parameters

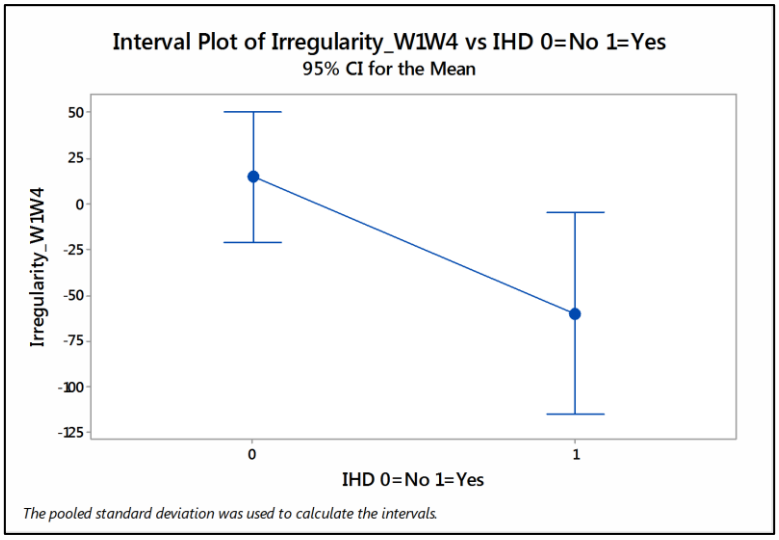

Figure 4.9: Interval plot of I_c (irregularity measure) with IHD (95% C.I. for the mean)

4.6.3 VLU contours

To investigate significant association between contour irregularity and healed status of VLUs in week 12, the I_c values were computed from five consecutive weeks' tracings and were considered for statistical analysis. Out of the total of 28 participants considered for analysis, there were 5 healed cases and 23 not-healed cases. The data was tested for normality using the Anderson-Darling test and it was found that the data did not follow a normal distribution. To test the hypothesis of whether the proposed method of irregularity holds any association with the healed status of the ulcers, non-parametric Kruskal Wallis test was performed on the I_c values.

The results obtained from Kruskal Wallis test have been tabulated in table 4.3 and the I_c values showed significant association with the healed status of the ulcers. Figure 4.10 shows the interval plot of I_c with respect to IHD which shows that there is a significant difference between the means of the two categories of data. From the interval plot, the I_c values are less for healed cases compared to not-healed cases, which means that the healed ulcers were more irregular than the not-healed ones (as I_c is inversely proportional to irregularity).

Table 4.3: Results of Kruskal-Wallis test for irregularity of VLUs with the healing status for five weeks

	Label	Median area	Mean Rank	Z-value	H-value	*p*-value
Baseline week	Healed	0.4	8.2	-1.89	3.57	**0.036**
	Not healed	0.58	15.9	1.89		
Week 1	Healed	0.35	8.6	-1.77	3.13	**0.035**
	Not healed	0.55	15.8	1.77		
Week 2	Healed	0.34	8.2	-1.89	3.57	**0.039**
	Not healed	0.57	15.9	1.89		
Week 3	Healed	0.29	7.2	-2.19	4.79	**0.029**
	Not healed	0.61	16.1	2.19		
Week 4	Healed	0.31	7.6	-2.07	4.28	**0.039**
	Not healed	0.54	16.0	2.07		

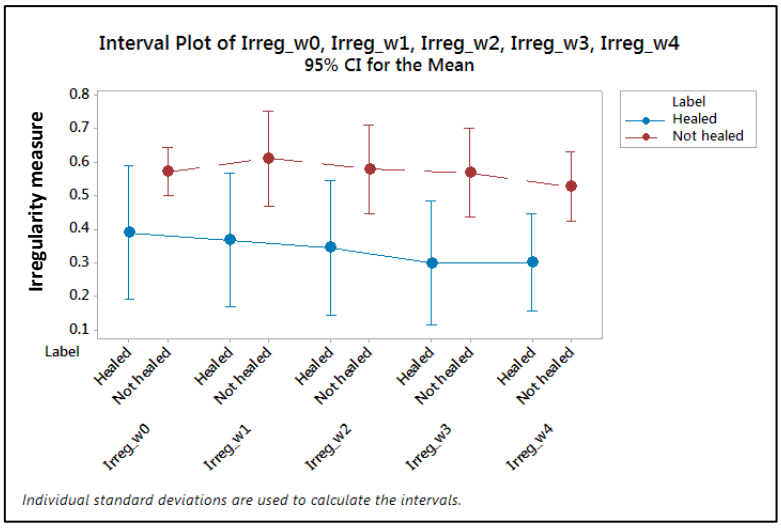

Figure 4.10: Interval plot of I_c (irregularity measure) with healed/ not-healed status (95% C.I. for the mean)

4.7 Summary

Fractal dimension (FD) has been used as an effective measure in description and characterization of complexity in the biological tissues which show self-similar properties (Carbonetto & Lew 2010; Jayalalitha & Uthayakumar 2007). The results obtained on synthetic images in this research work show that FD does not have a linear or even a monotonic relationship with noise value *n*, the factor indicative of the roughness or irregularity of the curves. This shows that FD is not suitable for estimating the irregularity or roughness of closed curves that were generated in this study as they are non-fractal curves. The analysis of the data shows that these curves cannot be fractals because there were insufficient data points and the fractal log-log curve is not sufficiently linear. This testing is essential because insufficient data points could lead to meaningless results and lack of linearity makes the estimation of irregularity based on FD incorrect. However, from literature, it is evident that this rigor has not been employed in most studies that have investigated the FD of biological tissues which indicates a significant weakness of earlier studies.

The irregularity or roughness of the synthetic curves generated in this work increase with the increase in the value of *n*, keeping all other factors constant. Visual inspection of the interval plot in figure 4.7(b) showed that I_c was associated with the changing values of *n*, and the linearity test in the mean values of I_c showed that the relationship was linear (R^2=0.99) with each *n*. The ANOVA result showed that there was significant difference between the values of I_c for different values of *n* which indicated that this index can differentiate between the curves generated using different values of *n*, having the trend with the curves corresponding to small values of *n* having the highest values of I_c. This could also be seen in the histogram plot in figure 4.8. The histogram showed normal distribution of the data, with each peak being distinct than the other for each value of *n*. Also, the I_c values increased with decrease in *n*, indicating inverse association with the irregularity of the curves. Thus, these results indicate that I_c can be used to quantify the irregularity of the curves.

To validate this method on biological tissues, contours of DFUs and VLUs were considered in this research work. Since diabetes is a multi-organ disease, healing of DFUs can be affected by other organ diseases as well as patients' medical conditions. Hence some of the important medical conditions such as IHD, PVD and CKD were considered for validation of the proposed method. The change in irregularity from week 1 to week 4 showed a good association with IHD. In other words, it was found that there was a significant change in contour irregularity for

participants with IHD, which is an important factor affecting the healing process of DFUs. This finding showed that there is significant association of the heart diseases of the patients with the irregularity of their ulcers, hence the patients with heart diseases should receive more serious intervention in the clinics for the treatment of their ulcers. The reason for consideration of week 4 data for the study of irregularity was that it holds clinical significance, since the clinical monitoring parameter is the fifty percent reduction of area of the ulcers from week 1 to week 4 for the ulcers to heal by week 12. Since FD is an effective way to measure the change in complexity with change in scale of any fractal object, it had also been computed to test its association with similar clinical conditions. However, unlike the proposed measure of irregularity, it did not show any association with any of the conditions, and therefore, it was not useful in the determination of complexity of ulcer contours.

In case of VLUs, the contours were obtained from the planimetry tracings and the I_c values calculated from the contours showed significant association with the healed status of the ulcers in week 12. It was also found that the I_c values were less for healed cases compared to not-healed cases, which indicated that the healed ulcers' contours were more irregular than the not-healed contours. Also, the irregularity increased over the consecutive weeks as the ulcers healed, while in not-healed contours, the irregularity decreased first and then increased over the five weeks' period. Thus, this method has been used for assessing the progress of ulcers through weeks, with irregularity of the contours as a measure of how much ulcers could evolve during the healing process. This means that the ulcers with more irregular contours could heal early (i.e. within the 12 weeks' time, hence classified as "healed"), whereas ulcers which show less irregularity in their contours would take longer time to heal, and would not heal within the 12 weeks' time, thus getting classified as "not-healed ulcers". It has also been successful in differentiating the healed ulcers from the not-healed ones. It should be noted that the ulcers which do not heal within the 12-week time period do require more serious intervention and longer follow-up time than 12 weeks.

The novelty of this work is that this index does not require the assumption that the curve is fractal and scale invariant. Strength of this index is that it does not require the specific selection of the position on the curve and is rotation invariant, which is important when investigating medical and natural objects. The proposed method can be used to quantify the irregularity or roughness of any curve or object contour without assuming the object to be fractal and having self-similar properties. This approach has the potential for several biological applications such as quantifying shapes of tumours and skin lesions, where the irregularity or roughness is

suitable for differentiating between malignant tumours from benign masses and skin melanoma cases from normal moles. Furthermore, in future, this parameter can also be used to help in predicting the healing trajectory of different type of ulcers.

Chapter 5

The association of temperature of diabetes -related foot ulcers with chronic kidney disorder

5.1 Introduction

The area of the diabetes related foot ulcer (DFU) and its reduction over weeks is used for assessment of the healing status of the ulcer in clinical practice; however, literature reports that this is not a reliable parameter as there can be multiple co-morbid diseases co-occurring with it, which are important factors affecting the healing of these ulcers and should be considered in their assessment. Thus, this work has investigated the use of thermal imaging and the association of change in the mean temperature of the ulcers with three clinical conditions relevant to ulcer healing, i.e. peripheral vascular disease (PVD), chronic kidney disease (CKD) and ischemic heart disease (IHD). Thermal and RGB images of 23 DFUs of the first two weeks of ulceration were studied. The potential application of this work is to show that the temperature obtained from thermal images of the ulcers can be used as a prognostic parameter for its assessment.

In this chapter, *section 5.2* highlights the use of thermal imaging in the risk assessment of developing ulcers in DFUs and the importance of co-morbid diseases in the healing of these ulcers. *Section 5.3* describes the database for validation of the proposed method. *Section 5.4* describes the method for segmentation of contours of the ulcers from RGB images using Snakes model for comparison with the proposed method. *Section 5.5* describes the proposed method of segmentation of ulcer contour from thermal images using Chan-Vese model. *Section 5.6* discusses the computation of area of the ulcer region from RGB images and mean temperature of the ulcer region from thermal images. S*ection 5.7* discusses the results obtained after statistical analysis on the association of area and mean temperature with the clinical conditions. Finally, *section 5.8* summarizes the main outcomes, advantages and prospective of this research work.

5.2 Thermal imaging of DFUs- literature review

Diabetes-related foot ulcers (DFUs) are serious complications in diabetic patients. Lack of effective intervention directed towards healing of the ulcers can lead to foot or lower limb amputation and even morbidity in extreme cases (Zimny, Schatz & Pfohl 2002). Assessment of these ulcers largely relies on visual inspection of the wound bed for size, shape and depth by expert clinicians (Paul et al. 2015; Sheehan et al. 2003).

For the assessment of the ulcers on a practical basis, the only clinical parameter is the area of the ulcers and their reduction over weeks (Warriner, Snyder & Cardinal 2011). However, there might be error in the measurement of area because of the presence of callus or other dead cells which might be present on the ulcer due to poor debridement, and the actual area of the ulcer might not be visible to measure. Moreover, the area might show reduction on the outside, but might have inflammation on the inside, whose effects would be seen in the following weeks.

Technologies such as thermal imaging can be used to assess the severity of the ulcers as it provides the underlying temperature distribution of the ulcers in a rapid, non-contact and non-invasive manner (Paul et al. 2015; Ring 2010). Thermal imaging has been used several times to assess the risk of developing DFUs and to assess reduced peripheral blood perfusion and ischemic conditions in the feet (Hernandez-Contreras et al. 2015; Houghton, Bower & Chant 2013; Mendes et al. 2015). The basic theory which has been used in literature is that an increase in skin temperature in one foot might have risk of ulceration as compared to its contralateral foot- the increase in temperature might be due to underlying inflammation (Houghton, Bower & Chant 2013). Thus, to assess the risk of developing ulcers in literature, thermal images of the feet were taken, and asymmetry analysis of subtracting the intensity levels (which correspond to the temperature values) of the ipsilateral foot from the corresponding intensity levels of the contralateral foot was performed. If the difference exceeded a set threshold of 2.2 degrees Celsius, the intensity was considered as a sign of abnormality (Houghton, Bower & Chant 2013; Liu et al. 2015; van Netten et al. 2013). Similar studies have been done with the case and control to identify high risk ulcer prone areas in diabetic patients (Macdonald et al. 2016; Pradhan & Kariyappa 2016).

While the prediction of risk of ulceration using thermal imaging has been widely studied, there have been very few works with the use of thermal imaging to study the open ulcers and their association with clinical conditions and healing. In this work, segmentation of the ulcer from the thermal images has been proposed using Chan-Vese model, which has not been implemented

for ulcer segmentation previously. The rationale behind this work is that the increase in temperature of the ulcers can be associated with increased inflammation, resulting in delayed healing; delayed healing is caused in patients suffering from some major clinical conditions too. Thus, the aim of this research work is to study the association between the mean temperature of the segmented ulcer obtained from the thermal imaging and the three clinical conditions associated with healing- CKD, PVD and IHD. For comparison, segmentation of the ulcer from RGB images for first two weeks and measurement of the area has also been performed.

5.3 Dataset for validation

The dataset used for this study was collected from the participants with type II diabetes who attended Austin Health, Melbourne for the treatment of their ulcers. Thermal and RGB images of the ulcers from 23 participants with age of 30 and over were used in this study. The images of the ulcers were taken using Fluke TiR1 thermal imaging camera. This camera saves images in both visible and infrared regions of the spectrum which allows direct comparison of RGB and thermal images (shown in figure 5.1). The room temperature and humidity were maintained constant while taking the thermal images, to avoid their effect on the study.

The data collection was performed by Biosignals Lab at RMIT and was provided to me for image analysis. The images obtained in the first two weeks of ulceration were used in this work to study the association between the change in mean temperature of the segmented ulcer in two consecutive weeks obtained from thermal imaging. Clinical data, i.e. IHD and PVD labels and estimated glomerular filtration rate (eGFR) levels of the participants were obtained from the hospital database. The eGFR is a measure of how well the kidneys filter the waste from blood and gives the best overall measure of the kidney function. The participants with eGFR<60ml/min per 1.73 m^2 were considered as the ones affected with CKD, as suggested by clinicians. This study was approved by the Human Research Ethics Committee (HREC) of Austin Health, University of Melbourne and RMIT University, Melbourne. All the ulcers received proper debridement prior to photography. In figure 5.1(b), the temperature of the ulcer region (wound bed) is different than the other regions of the foot, which confirms the importance of temperature in the assessment of ulcers.

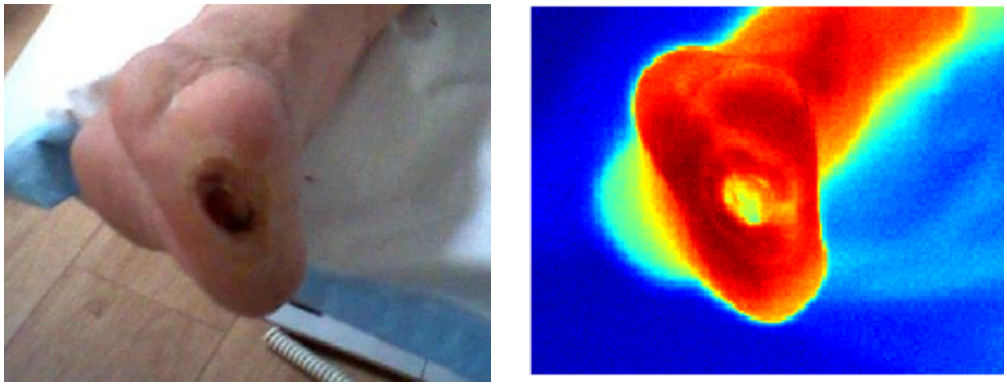

(a) (b)

Figure 5.1: (a) RGB image and (b) Thermal image of an ulcer- shows the change in the temperature of the ulcer region from the other regions of the foot

5.4 Segmentation of ulcer contours from RGB images using Snakes model

The RGB images were considered to compare with the proposed method as it is the widely accepted method for imaging of ulcers. The comparison was also made to show that the area obtained from RGB was different than the area obtained from thermal images. It is important to show that the areas obtained using the two imaging modalities are not the same, as it highlights the fact that the information obtained from thermal imaging is different and gives more information than the information obtained from RGB imaging. The segmentation of ulcer contours from RGB images was done using Snakes active contour model (Hettiarachchi et al. 2013; Kass, Witkin & Terzopoulos 1988). The snakes model used here is the same as the one used previously in this thesis, so refer to section 4.4.2.2 for more details on this algorithm. Figure 5.2(a) shows the evolving ulcer contour (in red), and figure 5.2(b) shows the final segmented contour.

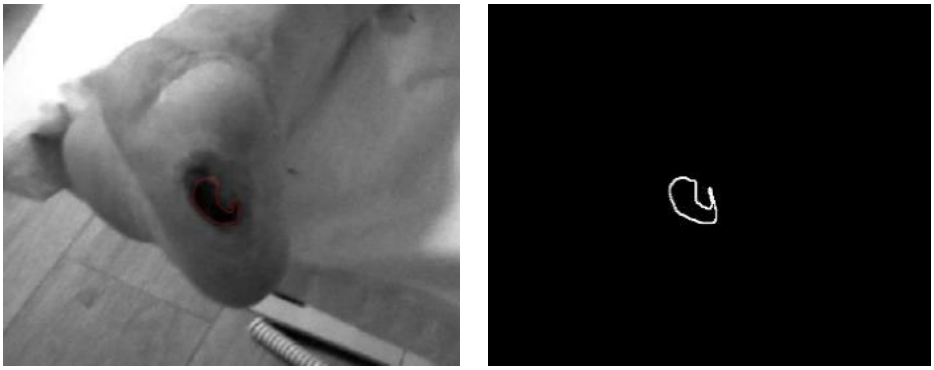

(a) (b)

Figure 5.2: (a) Grayscale image of the ulcer with the detected contour (in red) using Snakes model (b) Segmented contour

5.5 Segmentation of ulcer contour from thermal images using Chan-Vese model

As discussed in the previous section, Snakes model depends on the magnitude of gradient of the image to fit the iterating curve on the boundary of the object. In thermal images, the objects' boundaries are not defined by gradient and are smooth; hence Snakes model fails to work on these images. Thus, in this work, Chan-Vese active contour model has been proposed for segmentation of ulcers from thermal images for the first time, which performs global segmentation of the image and does not depend on local information (gradient) as the stopping criteria.

The Chan-Vese model is energy-based segmentation method and is based on Mumford-Shah segmentation and level set method. It works on minimizing the energy which is considered as a particular case of minimal partition problem, i.e., to partition the image into two subsets (two corresponding regions) such that the difference between the sum of elements in first subset and the sum of elements in second subset is minimized, where the evolving active contour divides the two corresponding regions- the inside region represents the object to be detected and the outside region represents the background (Chan & Vese 2001). The open access MATLAB code of the algorithm was used to implement the model.

To locate the ulcer region accurately, the RGB image was superimposed on the corresponding thermal image, as the thermal image has poor resolution and does not show the ulcer region clearly. The superimposition with RGB ensured that the ulcer region was correctly identified

on the thermal image and the points for segmentation were marked (figure 5.3(b)). The algorithm iterated on the thermal image, marking the contour of the ulcer when the algorithm reached its global minima. It should be noted that the ulcer region given by this model differs from the region seen in RGB images. This is because this algorithm works on segmenting the region based on temperature distribution and not the region defined by gradient. This is desirable as it shows the importance of underlying temperature distribution in the ulcers which is not visible in the respective RGB images. Figure 5.3(c) shows the detected ulcer region by the model, and the temperature inside the detected region is lower than the temperature outside the region.

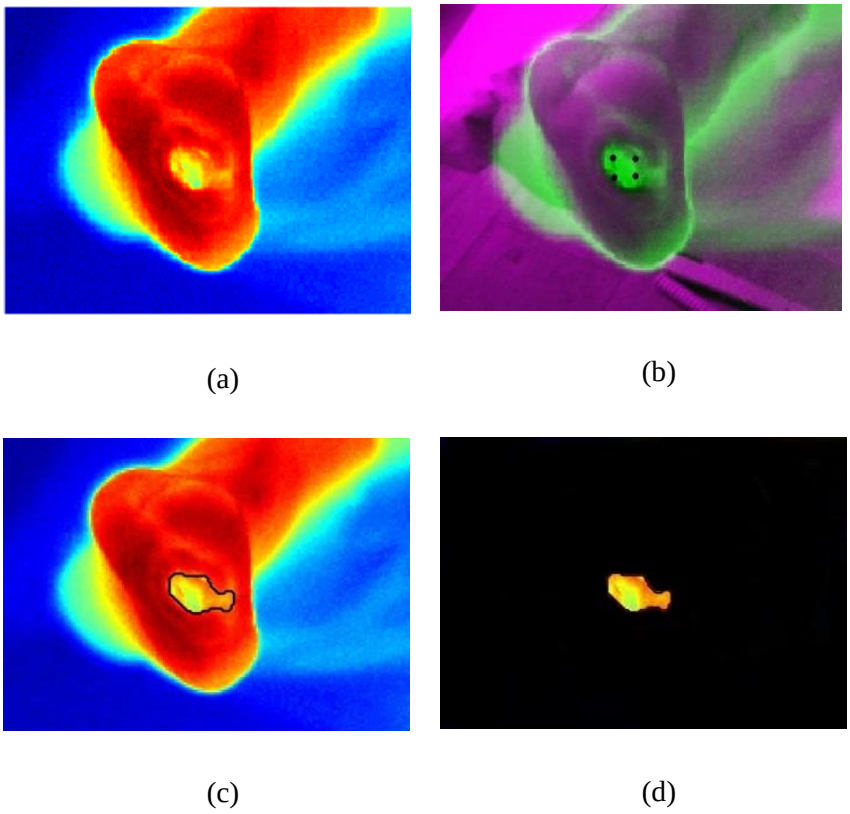

(a) (b)

(c) (d)

Figure 5.3: (a) Thermal image of the foot with ulcer, (b) Thermal image superimposed on the RGB image to detect the ulcer region accurately, (c) The detected ulcer region using Chan-Vese model, (d) The segmented ulcer region

5.6 Calculation of mean temperature and area

After the ulcer regions from thermal images were obtained, the mean temperature of the segmented ulcer region (shown in figure 5.3(d)) was measured. The area of the segmented ulcer region from RGB images (shown in figure 5.2(b)) was also obtained. The difference between the week 2 and week 1 values for both the parameters was calculated to measure the change in

the mean temperature and area from week 1 to week 2. These values were considered for statistical analysis to test the hypothesis, "the change in mean temperature shows association with any of the three clinical conditions i.e. CKD, PVD and IHD". The area of the ulcer was obtained from RGB images and was used to compare against the proposed method as the change in visible area obtained from RGB images is the current assessment technique. The data (change in mean temperature and the change in area) was tested for normality using Anderson-Darling test. To test the hypothesis, one-way ANOVA was performed using Fischer's exact method.

5.7 Results

The change in mean temperature and the change in area were found to follow normal distribution with *p*-value of 0.09 and 0.07 respectively. Out of the total of 23 participants considered for this study, the number of participants affected with IHD were 7, with PVD were 12 and with CKD were 12. The ANOVA results have been tabulated in table 5.1, which shows the *p*-values obtained for different clinical conditions and 95% C.I. for the mean difference between week 2 and week 1 parameters.

Table 5.1: Results obtained from ANOVA showing *p*-values, mean and confidence interval (C.I.) values for mean temperature (obtained from thermal images) and area (obtained from RGB images) with the clinical conditions

Clinical conditions		**Mean temp***	**Area***
CKD	***p-value***	**0.009**	0.554
	95% CI	**(0.26, 4.75)**	(-10748, 11285)
	mean	**2.50**	268
PVD	***p-value***	0.342	0.251
	95% CI	(-1.65, 3.09)	(-8884, 8365)
	mean	0.72	-260
IHD	***p-value***	0.593	0.497
	95% CI	(-2.34, 3.62)	(-11035, 10892)
	mean	0.64	-72

* the reported values correspond to the difference between week 2 and week 1 mean temperature and area

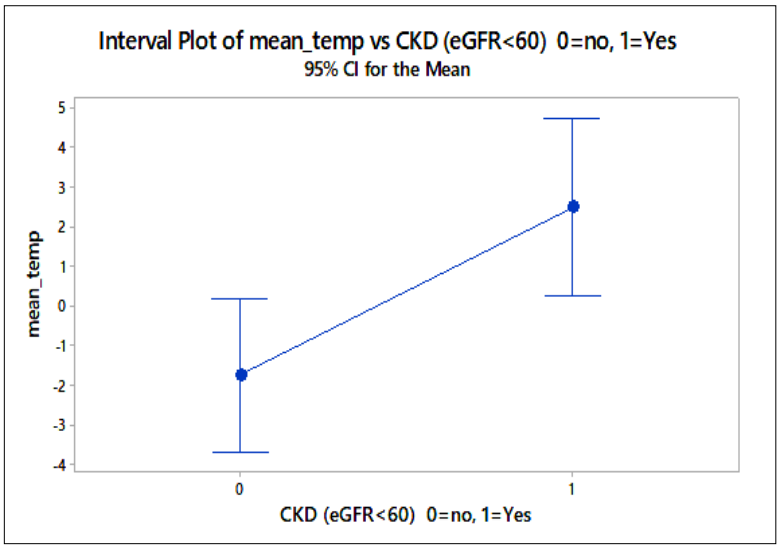

Figure 5.4: Interval plot showing significant difference between the change in mean temperature (from week 2 to week 1) and presence of CKD in the subjects

The change in mean temperature showed significant association with CKD as an important factor affecting the healing of ulcers (*p*-value of 0.009), while change in area measured from RGB images showed no significant association with any of the clinical conditions. Figure 5.4 showed the interval plot of the change in mean temperature with respect to CKD and showed the significant difference between the means of the temperature values in the two cases. It also showed that the mean temperature from week 1 to week 2 increased in participants affected with CKD while it decreased in participants not affected with CKD. The other two clinical conditions, namely IHD and PVD did not show association with the change in mean temperature nor with the change in area of the ulcers.

5.8 Summary

This research work proposed the use of temperature of the ulcers as one of the prognostic parameters to be used in the assessment of healing status of the ulcers. Since diabetes is a multi-organ systemic disease, the healing of the ulcers is dependent on the diseases co-occurring in the patients; hence this study investigated the association of the mean temperature of the ulcers with the clinical conditions.

The three main clinical conditions which are known to affect the healing of ulcers were considered in this work: IHD, PVD and CKD. The change in the mean temperature of the ulcer region from week 1 to week 2 were considered to test against the clinical conditions so that the factors associated with delayed healing could be identified in the early stages of the ulcer. For

comparison, the current method of assessment of the ulcers which is based on the area of the ulcer was considered and the area was obtained from RGB images. The results showed that while the area of the ulcer was not a good indicator of the associated clinical conditions, the weekly change in the temperature of the ulcer was significantly higher in participants with CKD.

The novelty of this work is that it has shown significant association of mean temperature with CKD, an important clinical condition affecting the healing of the ulcers. It is observed that in participants not affected with CKD, the temperature in week 2 reduced compared to week 1 which indicates reduced inflammation in week 2, while the mean temperature of participants with CKD increased from week 1 to week 2, which could indicate increased inflammation in week 2 than week 1.

This work shows the use of thermal imaging to study the change in the temperature distribution of the DFUs in the first two weeks. CKD is one of the important clinical conditions affecting the healing of the ulcers, and the change in the mean temperature of the ulcers has shown significant association with CKD. The limitation of this work is that the healing status of the ulcers has not been studied. However, this work shows the potential of thermal imaging to be used to study the healing status of the ulcers in twelve weeks period and temperature can be studied as one of the prognostic parameters to assess the healing status of the ulcers, as has been done in one of the collaborative studies (Aliahmad et al. 2018).

Chapter 6

Classification of healed and not-healed venous leg ulcers using thermal imaging technique

6.1 Introduction

Venous leg ulcers (VLUs) are the most common type of chronic wounds and are a major cause of pain and disability, especially in the elderly people. They are caused by venous obstruction or reflux, which leads to poor venous return (poor return of blood from legs to the heart) and venous hypertension (increased pressure in the veins). These ulcers also have negative impact on the quality of lives of people affected with them, also leading to high rate of mortality among patients.

In this chapter, thermal imaging technique for measurement of area of the ulcers has been proposed and tested to differentiate between the healed and not-healed cases and predict the healing status of the ulcers. For comparison, the currently used digital planimetry technique for measurement of area has been tested for significance of prediction of the healing status of the ulcers. In this chapter, *section 6.2* highlights the importance of digital planimetry technique for measurement of area of the ulcers and addresses its limitations. It also gives a review on the use of thermal imaging and its advantages on the assessment of ulcers. *Section 6.3* describes the database of VLUs which has been used for validation of the method. *Section 6.4* describes the method used for segmentation of ulcers from thermal images and measurement of the corresponding area of the ulcers. *Section 6.5* describes the results obtained from the area of digital planimetry technique, its limitations and the results obtained from the area of thermal imaging and discusses how thermal imaging is a better technique for assessment and prediction of the healing status of the ulcers compared to digital planimetry technique. Finally, *section 6.6* summarizes the main outcomes and advantages of the proposed method.

6.2 Digital planimetry and thermal imaging of ulcers

One of the accurate assessment techniques widely used in the assessment of the ulcers is using digital planimetry technique, which has been discussed in detail in section 2.4. The ulcers usually have underlying inflammation in them, characterised by redness, swelling, heat and pain. These signs may be difficult to assess objectively from outside by visual inspection by clinicians (Kaabouch et al. 2010). It has been reported that other parameters such as the temperature of the ulcers and the surrounding regions can provide quantitative information about the inflammation and the healing status of the ulcers. Thermal imaging is a rapid, non-invasive and non-contact imaging technique which has been discussed in detail in section 2.4 and 5.2.

With respect to work in thermal imaging and open ulcers, it has been reported that the temperature measurement can provide useful objective information about the healing progress of the ulcers, as the presence of higher local temperature can be related to inflammation or infection, while the presence of lower temperature can indicate a slow healing rate, mainly owing to decrease in oxygen in that region (Barone, Paoli & Razionale 2011). In one of the works, the advantage of thermal imaging on assessment of chronic ulcers was studied where the integration of stereo vision system with infrared detector was used to combine the colour and thermal imaging to obtain both colour texture and temperature information (Barone, Paoli & Razionale 2011). These 2D results were projected onto 3D models and automatic measurement of volumetric parameters of the wounds were performed. Another study used thermal imaging as one of the tools to monitor the changes in the characteristics of blood flow and metabolic processes as the wound progresses (Chen, MH et al. 2005). However, no work has been done to study the healing trajectory of the ulcers based on the area of the ulcers with respect to the temperature distribution in them.

The hypothesis of this study is that thermal imaging can predict the healing trajectory of venous leg ulcers better than digital planimetry technique. In other words, the area obtained from the temperature distribution of the wound using thermal imaging would be a better predictive measure than the wound surface area measured using digital planimetry technique and can differentiate between the healed and not-healed ulcers.

6.3 Dataset for validation

All individuals aged 18 years or above with leg ulcers being attended by Bolton Clarke, Melbourne, Australia were recruited in this study. The inclusion criteria were presence of venous leg ulcers, with Ankle Brachial Pressure Index between 0.8-1.2 and having signs of venous diseases using clinical, aetiological, anatomical and pathological (CEAP) classification system (Rabe & Pannier 2012). The ulcers from the ankle region to below the knee region were considered in this study. A total of 36 participants who satisfied the above inclusion criteria were considered for this study.

The data collection was performed by the nursing staff of Bolton Clarke who attended the participants in their homes to provide care and treatment for the ulcers, and the image processing of the data was performed by me. Thermal images for five consecutive weeks were collected; the first week being considered as baseline, followed by four consecutive weeks. Initial clinical assessment was done for all participants in the baseline week- demographic information, comorbidities information and wound related information were obtained. All the ulcers received standard wound care from the baseline week until the ulcers healed. The images were taken by a trained research nurse to maintain consistency in data collection. The RGB images were also collected to provide reference for the location of the ulcers. Figure 6.1 shows the RGB image and the respective thermal image of a venous leg ulcer.

These ulcers were weekly attended by the nurse to provide care in terms of appropriate dressings and effective compression. The area of the ulcers was also obtained in each week using digital planimetry technique as standard clinical practice to assess the healing status of the ulcers which has also been considered in the analysis. This study was approved by Human Research and Ethics Committee of Boston Clarke and RMIT University and written consents of the participants were also obtained in the baseline week for the study.

(a) (b)

Figure 6.1: (a) RGB image and (b) Thermal image on a venous leg ulcer

6.4 Segmentation of ulcer contour from thermal images

The analysis of the images so collected was performed by me and I have considered all five weeks of thermal images obtained from 36 ulcers for measurement of area of the ulcers. Since the images were taken in different weeks at different times, there were slight changes in their orientation and scale. Hence the images of the follow-up weeks were registered with the baseline week images to remove the variance in orientation and scale. To perform the registration, Image Registration toolbox available in MATLAB was used which uses salient features of the image as reference to perform registration, refer to section 4.4.2.1 for more details on the algorithm. In the case of VLU images, the edges of the legs were considered as reference. Figure 6.2 shows the original images of two weeks and their respective registered images.

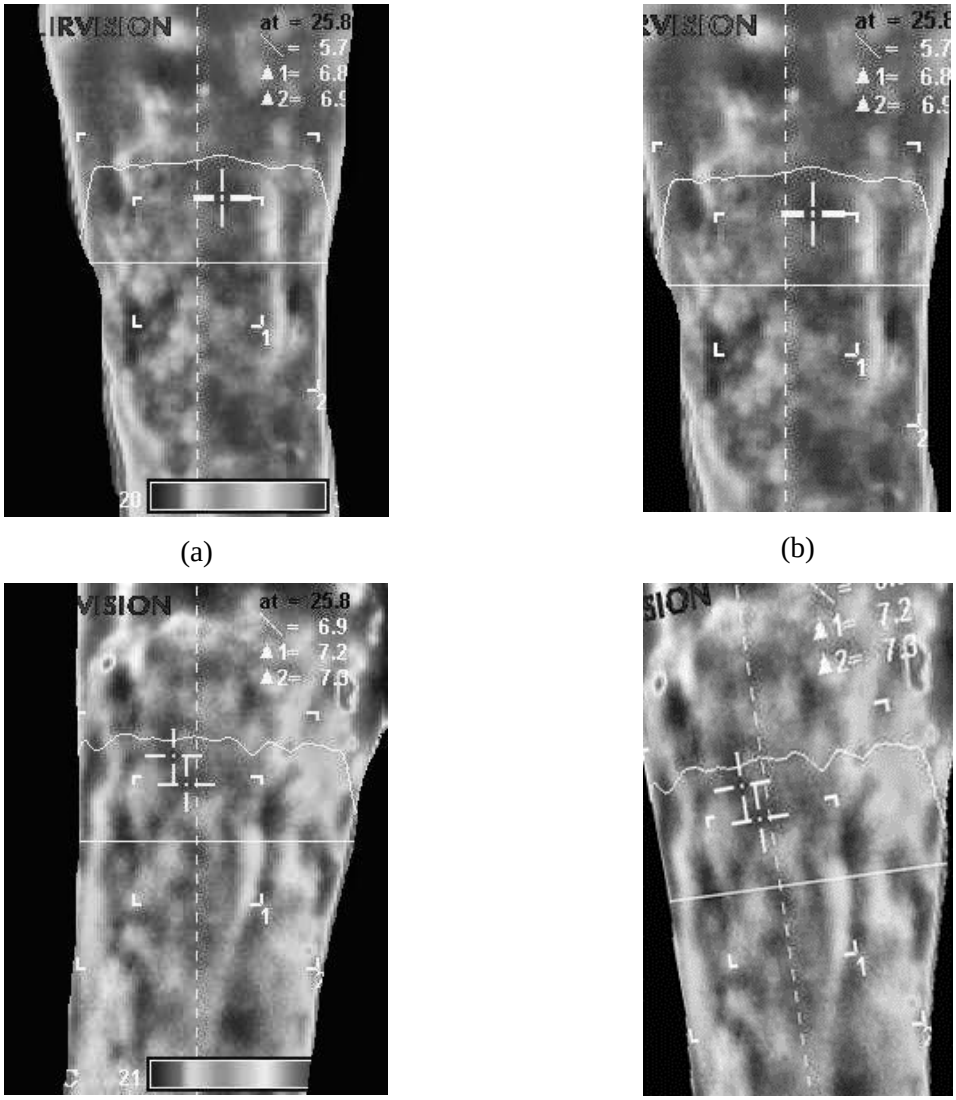

(a) (b)

(c) (d)

Figure 6.2: (a) Week 0 original image, (b) Week 0 registered image, (c) Week 1 original image (d) Week 1 registered image

To enhance the contrast of the ulcer region from the other regions of the leg, pre-processing using histogram equalization was performed, which adjusts the image intensity values to enhance the contrast of the image. Figure 6.3(a) shows the obtained thermal image from the thermal camera while figure 6.3(b) shows the effect of contrast enhancement, where the wound region can be clearly seen enhanced than the other leg regions. Segmentation of the enhanced wound region was performed using Chan-Vese segmentation model (Chan & Vese 2001), which is a common active contour segmentation model used for segmentation, especially in case of images obtained with low resolution imaging techniques such as thermal imaging, where the edges of the objects of interest are not clearly defined (figure 6.3(c)). It has been previously used on brain MRI images for segmentation of tumours and segmentation of white

matter (Crandall 2009; Wu, Hou & Wu 2011). Reference can be made to section 5.5 for more details on this algorithm.

For comparison with thermal image, RGB image of the ulcer has been shown in figure 6.3(d) to show how the ulcer looks on the surface, and its area traced using digital planimetry (figure 6.3(e)). It can be seen in the figure that the shape and the area obtained from thermal images based on the temperature distribution (figure 6.3(c)) is very different from the shape and surface area obtained using digital planimetry (figure 6.3(f)). After the segmented ulcer region based on temperature distribution was obtained, the area of the bounded region was calculated using MATLAB.

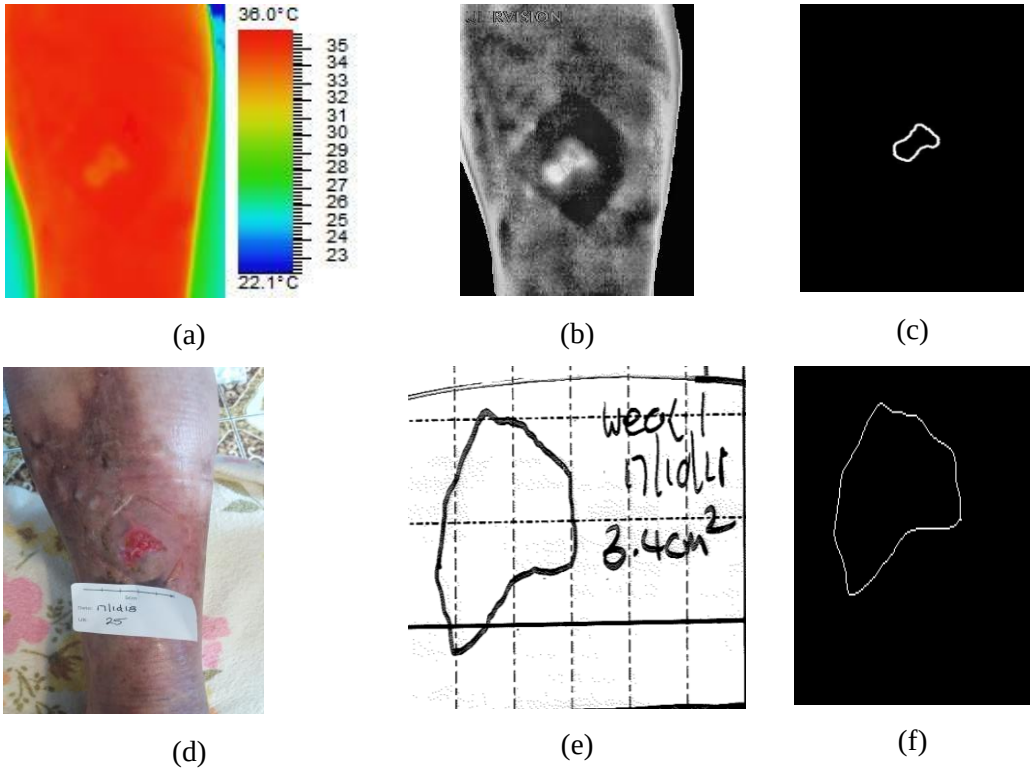

(a) (b) (c)

(d) (e) (f)

Figure 6.3: (a) Thermal image (b) After preprocessing (c) Segmented ulcer region (d) RGB image showing the ulcer on skin surface (e) Wound tracing (f) Ulcer region after tracing

6.5 Results

The area obtained from digital planimetry and thermal imaging were tested for normality using the Anderson-Darling test and it was found that they did not follow normal distribution. Hence non-parametric Kruskal Wallis test was performed to test the association of area of five consecutive weeks with the healed status of the ulcers, since it is the equivalent test of the

parametric ANOVA test. The interval plots of the area with 95% confidence interval (C.I.) were also obtained to study the distribution of the area in the healed and not-healed cases.

Table 6.1 summarises the statistical results from the area obtained using digital planimetry. Out of the total of 36 ulcers, the number of healed cases were 7 and the number of not-healed cases were 29. It can be seen that the area of all the five weeks showed significant association with the healed/not-healed status obtained in week 12. Figure 6.4 shows the interval plots of the healed vs. not healed for 95% C.I. cases, and it can be seen that all the healed cases had significantly smaller areas (<5cm^2) compared to the not-healed cases, whose areas were quite high. However, it can also be seen that there is an overlap in the interval plots between the healed and not-healed cases, as all the ulcers that were small did not fall into the healed category.

Table 6.1: Results of Kruskal-Wallis test for area of VLUs obtained using digital planimetry with the healed status for five weeks

	Label	**Median area**	**Mean Rank**	**Z-value**	**H-value**	***p*-value**
Baseline week	Healed	0.9	8.3	-2.8	7.86	**0.005**
	Not healed	0.5	20.4	2.8		
Week 1	Healed	1	8.8	-2.6	6.75	**0.009**
	Not healed	5.6	19.8	2.6		
Week 2	Healed	0.3	7.8	-2.32	5.36	**0.021**
	Not healed	5.5	16.9	2.32		
Week 3	Healed	0.35	8.7	-2.33	5.45	**0.022**
	Not healed	5.20	18.9	2.33		
Week 4	Healed	0.1	8.2	-2.88	8.28	**0.004**
	Not healed	5.0	21.0	2.88		

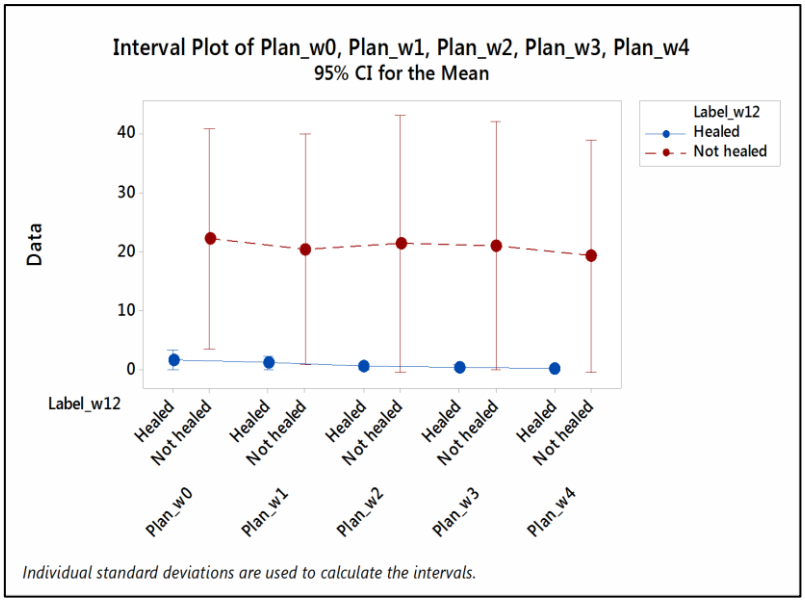

Figure 6.4: Interval plots showing significant difference between area of healed and not-healed ulcers for five weeks

Table 6.2 summarises the results from the area obtained using thermal imaging. All the five weeks of area showed significant association with the healed/ not-healed status of the ulcers obtained in week 12. Figure 6.5 shows the interval plots of the 95% C.I. in both cases, and there is no overlap between the intervals of healed and not-healed cases. Hence the ulcers having small areas healed while the ulcers having larger areas (as seen in the thermal images) did not heal in the twelve weeks' time.

Table 6.2: Results of Kruskal-Wallis test for area of VLUs obtained using thermal imaging with the healed status for five weeks

	Label	Median area	Mean Rank	Z-value	H-value	*p*-value
Baseline week	Healed	4071.3	6.4	-3.38	11.41	0.001
	Not healed	16966.1	21.4	3.38		
Week 1	Healed	2061.1	5.4	-3.66	13.38	<0.001
	Not healed	18457.5	21.7	3.66		
Week 2	Healed	4146.6	6.4	-3.38	11.41	0.001
	Not healed	17723.5	21.4	3.38		
Week 3	Healed	2838.9	4.9	-3.82	14.57	<0.001
	Not healed	16984.0	21.8	3.82		
Week 4	Healed	4507.8	6.6	-3.34	11.14	0.001
	Not healed	15565.3	21.4	3.34		

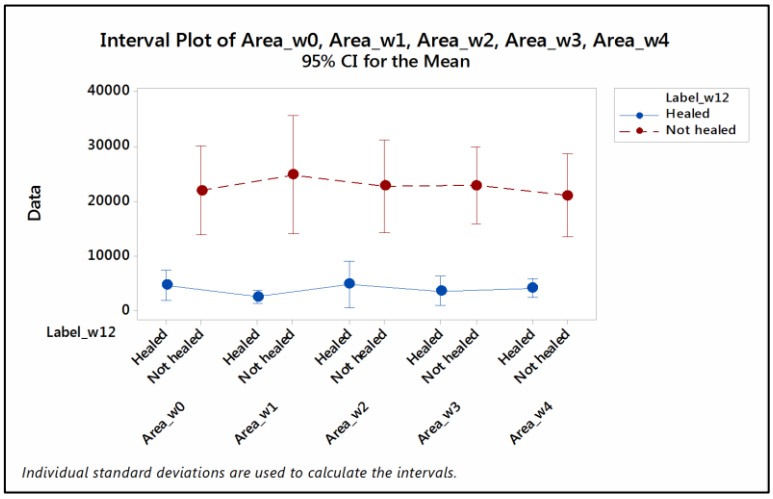

Figure 6.5: Interval plots showing significant difference between area of healed and not-healed ulcers for five weeks

6.6 Summary

Digital planimetry is a widely used technique to measure the area of the ulcers and to assess the healing status of the ulcers. Hence this work considered the use of planimetry to measure the area of the ulcers. However, since healing of ulcers is a multi-factorial process,

measurement of surface area of the ulcers is not a reliable parameter as there are certain other objective parameters which should be considered for assessment, such as the depth of the ulcers, temperature of the ulcers, etc. In this work, the temperature of the ulcers was considered to test the hypothesis that the area obtained using temperature distribution of the ulcers can be used for prediction of the healing status of venous leg ulcers.

The results obtained using thermal imaging showed that the healed ulcers were significantly smaller in area (obtained using temperature distribution of the ulcers) than the not-healed cases (figure 6.5). This was supported by the significance level which was also quite high as seen from lower *p*-values (*p*-value of 0.001 or <0.001, as seen in table 6.2) compared to the area using digital planimetry (*p*-value of 0.004 and higher, as seen in table 6.1). This was further seen in the interval plots where the overlap between the intervals of the healed and not-healed was seen (figure 6.4), which suggested that even though all the healed cases had smaller areas, all the ulcers with smaller area did not end up healing by the end of twelve weeks. Thus, the novelty of this work is that the area obtained using thermal imaging is a better predictor of healing status of the ulcers than the digital planimetry technique. While the difference between the two methods was quite small and digital planimetry is the accepted assessment technique, it is not a convenient method as it requires contact with the ulcers while thermal imaging is a non-contact and non-invasive method.

It can be observed that the ulcers with larger baseline areas would need longer time to heal and hence would require longer follow-up than 12 weeks. It can be further observed that since the thermal area of all five weeks showed significant association with the healed status of the ulcers, the area obtained in the baseline week alone can also predict the healing trajectory of the ulcers. This would lead to better monitoring of the ulcers from the baseline week itself, as the clinicians do not need to wait for four more weeks to conclude on the healing trajectory of the ulcers.

Chapter 7

Conclusion

This research work has examined the novel objective parameters for assessment and prediction of the healing status of the diabetes-related foot ulcers (DFUs) and venous leg ulcers (VLUs). This work has demonstrated that the current clinical monitoring parameter for the assessment of ulcers by considering reduction in ulcers' area by 50% within 4 weeks of treatment is not a reliable measure. This thesis has developed new methods to quantify alternative objective measures for better assessment of the healing status of ulcers. It has also demonstrated the importance of associated clinical conditions with the healing status, thus proving quantitatively that healing of chronic ulcers is a multi-factorial process.

This work has developed an irregularity index (I_c) to quantify curve irregularity by measuring the change in the roughness of the segments of the curve with change in window sizes. The proposed index has been validated using synthetically generated curves having different degrees of roughness and the results showed linear relationship of the index with the roughness level. It has also demonstrated that fractal dimension, the method widely used in literature for quantification of irregularity, did not show any association with the roughness level. Thus, this work has concluded using statistical significance test that I_c values showed significant difference among the six different groups of curves with varying irregularity.

This work has also validated the above method on DFUs and VLUs. Diabetes is a multi-organ systemic disease, and healing of DFUs can be affected by other organ diseases as well as patients' medical conditions. This work has demonstrated a significant change in the irregularity of the ulcer contour from week 1 to week 4 in the presence of ischemic heart disease, which is an important factor affecting the healing of DFUs. Hence the patients with heart diseases should receive more serious intervention in the clinics for the treatment of their ulcers. In case of VLUs, this work has considered the contours obtained from the digital planimetry tracings and the I_c values calculated from the contours have shown significant association with the healed status of the ulcers in week 12.

This research work has investigated the use of temperature of the ulcers as one of the prognostic parameters to be used in the assessment of healing status of the ulcers. The change in the mean

temperature of the ulcer region from week 1 to week 2 were considered to test against the clinical conditions so that the factors associated with delayed healing could be identified in the early stages of the ulcer. For comparison, the current method of assessment of the ulcers based on the area of the ulcer from RGB images was also considered. The results have demonstrated that while the area of the ulcer from RGB images is not a good indicator of the associated clinical conditions, the weekly change in the temperature of the ulcer is significantly higher in subjects with Chronic Kidney Disorder (CKD) than the ones not affected with CKD.

Last but not the least, this study has also demonstrated the significant association of the area obtained using thermal imaging and the healed status of the VLUs. The results have shown that the healed ulcers were significantly smaller in area (obtained using temperature distribution of the ulcers) than the not-healed ones, while the results obtained from the area using digital planimetry didn't show the same level of significance. Thus, this work concluded that the area obtained using thermal imaging is a better predictor of the healing status of ulcers than the digital planimetry technique.

7.1 Main contributions of the thesis

This thesis reports my research work that was done in partnership with clinicians from Austin Hospital and Bolton Clarke, Melbourne. The main contributions of the thesis are as follows:

- This work has proposed a novel method for quantification of irregularity in curves which do not exhibit self-similar properties. It was validated on synthetic curves with varying levels of irregularity (published in Physica A: Statistical Mechanics and its Applications, 2019 (Rani, P, Aliahmad & Kumar 2019)).
- This work has demonstrated the quantification of irregularity in the contours to study the properties of ulcer contours and their association with co-morbid diseases in diabetes-related foot ulcers (published in the proceedings of IEEE Engineering in Medicine and Biology Conference (EMBC), 2017 (Rani, P, Aliahmad & Kumar 2017)) and the healed status of venous leg ulcers. The novelty of this work is that this index does not assume the curve to be fractal and scale invariant. Strength of this index is that it does not require the specific selection of the position on the curve and is rotation invariant, which is important when investigating medical and natural objects.
- This work has demonstrated the significant association of mean temperature of diabetes-related foot ulcers with Chronic Kidney Disorder, an important clinical condition affecting the healing of the ulcers (published in IEEE Engineering in

Medicine and Biology Conference (EMBC), 2019 (Rani, P, Aliahmad, B and Kumar, DK 2019)).

- This work has differentiated between the healed and not-healed venous leg ulcers by investigating their area measured using different techniques (digital planimetry and thermal imaging) and it demonstrated that the area measured using thermal imaging is a better predictor of healing status of the ulcers than the digital planimetry technique.

7.2 Future studies

While this study has developed and validated the methods on DFUs and VLUs, it can be further extended and tested on other ulcers and wounds (such as burns) for assessment of their healing status. This study can further be conducted on increased number of participants as the total number of participants were within forty in this study. Apart from contour irregularity and temperature distribution, more parameters can be added to make the assessment of ulcers much better. Along with thermal imaging, hyperspectral imaging and stereo-imaging can also be tested on chronic ulcers to get additional information on parameters such as oxygen saturation of ulcers, depth of the ulcers, etc.

The methods developed in this thesis can find applications in similar diseases, such as different types of wounds, tumors, skin lesions, etc. The method for quantification of irregularity can be extended to quantify irregularity of breast tumors and skin lesions since the irregularity of their contours is an important diagnostic parameter. Moreover, the approach on isothermal patches and the segmentation of area using thermal imaging can also be implemented on tumor images and skin lesion images for prediction and detection due to increase in temperature of the respective regions of the body.

References

'MATLAB and Image Processing Toolbox Release 2015a', 2015, *The MathWorks, Inc., Natick, Massachusetts, United States*.

Abbott, C, Carrington, A, Ashe, H, Bath, S, Every, L, Griffiths, J, Hann, A, Hussein, A, Jackson, N & Johnson, K 2002, 'The North-West Diabetes Foot Care Study: incidence of, and risk factors for, new diabetic foot ulceration in a community-based patient cohort', *Diabetic medicine*, vol. 19, no. 5, pp. 377-384.

Alhasan, A, White, DJ & De Brabanter, K 2016, 'Wavelet filter design for pavement roughness analysis', *Computer-Aided Civil and Infrastructure Engineering*, vol. 31, no. 12, pp. 907-920.

Aliahmad, B, Tint, AN, Poosapadi Arjunan, S, Rani, P, Kumar, DK, Miller, J, Zajac, JD, Wang, G & Ekinci, EI 2018, 'Is Thermal Imaging a Useful Predictor of the Healing Status of Diabetes-Related Foot Ulcers? A Pilot Study', *Journal of diabetes science and technology*, vol., p. 1932296818803115.

Andersen, H 2012, 'Motor dysfunction in diabetes', *Diabetes/metabolism research and reviews*, vol. 28, pp. 89-92.

Armstrong, DG, Boulton, AJ & Bus, SA 2017, 'Diabetic foot ulcers and their recurrence', *New England Journal of Medicine*, vol. 376, no. 24, pp. 2367-2375.

AWMA 2010, *Standards for Wound Management*, Australian Wound Management Association, <http://www.awma.com.au/publications/2011_standards_for_wound_management_v2.pdf>.

Bakker, K, Apelqvist, J, Schaper, NC & Board, IWGotDFE 2012, 'Practical guidelines on the management and prevention of the diabetic foot 2011', *Diabetes/metabolism research and reviews*, vol. 28, pp. 225-231.

Ballard, JL & Bergan, J 2012, *Chronic Venous Insufficiency: Diagnosis and Treatment*, Springer Science & Business Media.

Barone, S, Paoli, A & Razionale, AV 2011, 'Assessment of chronic wounds by three-dimensional optical imaging based on integrating geometrical, chromatic, and thermal data',

Proceedings of the Institution of Mechanical Engineers, Part H: Journal of Engineering in Medicine, vol. 225, no. 2, pp. 181-193.

Bernard, V, Staffa, E, Mornstein, V & Bourek, A 2013, 'Infrared camera assessment of skin surface temperature – Effect of emissivity', *Physica Medica*, vol. 29, no. 6, pp. 583-591.

Bharara, M, Cobb, J & Claremont, D 2006, 'Thermography and thermometry in the assessment of diabetic neuropathic foot: a case for furthering the role of thermal techniques', *The International Journal of Lower Extremity Wounds*, vol. 5, no. 4, pp. 250-260.

Boulton, AJ, Vileikyte, L, Ragnarson-Tennvall, G & Apelqvist, J 2005, 'The global burden of diabetic foot disease', *The Lancet*, vol. 366, no. 9498, pp. 1719-1724.

Boyko, EJ, Ahroni, JH, Stensel, V, Forsberg, RC, Davignon, DR & Smith, DG 1999, 'A prospective study of risk factors for diabetic foot ulcer. The Seattle Diabetic Foot Study', *Diabetes care*, vol. 22, no. 7, pp. 1036-1042.

Briggs, M & Nelson, E 2010, 'Topical agents or dressings for pain in venous leg ulcers', *Cochrane Database of Systematic Reviews*, vol. 4.

Carbonetto, SH and Lew, SE 2010, 'Characterization of border structure using fractal dimension in melanomas', *2010 Annual International Conference of the IEEE Engineering in Medicine and Biology* (pp. 4088-4091). IEEE.

Cardinal, M, Eisenbud, DE, Phillips, T & Harding, K 2008, 'Early healing rates and wound area measurements are reliable predictors of later complete wound closure', *Wound Repair & Regeneration*, vol. 16, no. 1, pp. 19-22.

Chan, TF & Vese, LA 2001, 'Active contours without edges', *IEEE Transactions on image processing*, vol. 10, no. 2, pp. 266-277.

Chang, AC, Dearman, B & Greenwood, JE 2011, 'A comparison of wound area measurement techniques: visitrak versus photography', *Eplasty*, vol. 11.

Chen, MH, Kerechanin, CW, Greenspan, DG, Criss, TB, Franckowiak, SC, Vincent, JA & Pattay, RS 2005, 'Development of a thermal and hyperspectral imaging system for wound characterization and metabolic correlation', *Johns Hopkins APL technical digest*, vol. 26, no. 1, pp. 67-74.

Chen, X, Raja, J & Simanapalli, S 1995, 'Multi-scale analysis of engineering surfaces', *International Journal of Machine Tools and Manufacture*, vol. 35, no. 2, pp. 231-238.

Coerper, S, Beckert, S, Küper, MA, Jekov, M & Königsrainer, A 2009, 'Fifty percent area reduction after 4 weeks of treatment is a reliable indicator for healing—analysis of a single-center cohort of 704 diabetic patients', *Journal of Diabetes and its Complications*, vol. 23, no. 1, pp. 49-53.

Coyer, FM, Edwards, HE & Finlayson, KJ 2005, *National Institute for Clinical Studies Report for Phase 1, Evidence Uptake Network : Best Practice Community Care for Clients with Chronic Venous Leg Ulcers*, Brisbane, Qld, <http://eprints.qut.edu.au/54240/2/54240.pdf>.

Crandall, R 2009, 'Image segmentation using the Chan-Vese algorithm', *Project report from ECE*, vol. 532.

Cutting, JE & Garvin, JJ 1987, 'Fractal curves and complexity', *Attention, Perception, & Psychophysics*, vol. 42, no. 4, pp. 365-370.

Davis, W, Norman, P, Bruce, D & Davis, T 2006, 'Predictors, consequences and costs of diabetes-related lower extremity amputation complicating type 2 diabetes: the Fremantle Diabetes Study', *Diabetologia*, vol. 49, no. 11, pp. 2634-2641.

Delbridge, L, Ctercteko, G, Fowler, C, Reeve, T & Le Quesne, L 1985, 'The aetiology of diabetic neuropathic ulceration of the foot', *British Journal of Surgery*, vol. 72, no. 1, pp. 1-6.

Dumville, J, Soares, M, O'meara, S & Cullum, N 2012, 'Systematic review and mixed treatment comparison: dressings to heal diabetic foot ulcers', *Diabetologia*, vol. 55, no. 7, pp. 1902-1910.

Edmonds, ME & Foster, A 2006, 'ABC of wound healing: Diabetic foot ulcers', *Student BMJ*, vol. 14.

Edwards, H, Finlayson, K, Courtney, M, Graves, N, Gibb, M & Parker, C 2013, 'Health service pathways for patients with chronic leg ulcers: identifying effective pathways for facilitation of evidence based wound care', *BMC Health Services Research*, vol. 13, no. 86.

Edwards, HE, Parker, CN, Miller, C, Gibb, M, Kapp, S, Ogrin, R, Anderson, J, Coleman, K, Smith, D & Finlayson, KJ 2018, 'Predicting delayed healing: The diagnostic accuracy of a

venous leg ulcer risk assessment tool', *International wound journal*, vol. 15, no. 2, pp. 258-265.

Fagervik-Morton, H & Price, P 2009, 'Chronic ulcers and everyday living: Patients' perspective in the UK', *Wounds*, vol. 21, no. 12, pp. 318-323.

Forssgren, A, Fransson, I & Nelzén, O 2008, 'Leg ulcer point prevalence can be decreased by broad-scale intervention: a follow-up cross-sectional study of a defined geographical population', *Acta Dermato-Venereologica*, vol. 88, no. 3, pp. 252-256.

Franks, P & Moffatt, C 2001, 'Health related quality of life in patients with venous ulceration: use of the Nottingham health profile.', *Quality of Life Research*, vol. 10, no. 8, pp. 693-700.

Gethin, G & Cowman, S 2006, 'Wound measurement comparing the use of acetate tracings and VisitrakTM digital planimetry', *Journal of clinical nursing*, vol. 15, no. 4, pp. 422-427.

Gonzato, G, Mulargia, F & Marzocchi, W 1998, 'Practical application of fractal analysis: problems and solutions', *Geophysical Journal International*, vol. 132, no. 2, pp. 275-282.

Górski, AZ & Skrzat, J 2006, 'Error estimation of the fractal dimension measurements of cranial sutures', *Journal of anatomy*, vol. 208, no. 3, pp. 353-359.

Greenman, RL, Panasyuk, S, Wang, X, Lyons, TE, Dinh, T, Longoria, L, Giurini, JM, Freeman, J, Khaodhiar, L & Veves, A 2005, 'Early changes in the skin microcirculation and muscle metabolism of the diabetic foot', *The Lancet*, vol. 366, no. 9498, pp. 1711-1717.

Grey, JE, Enoch, S & Harding, KG 2006, 'Wound assessment', *Bmj*, vol. 332, no. 7536, pp. 285-288.

Guo, Q, Ruiz, V, Shao, J and Guo, F 2005, 'A novel approach to mass abnormality detection in mammographic images', *Proceedings of the IASTED International Conference on Biomedical Engineering* (pp. 180-185).

Havlin, S, Buldyrev, S, Goldberger, A, Mantegna, R, Ossadnik, S, Peng, C-K, Simons, M & Stanley, H 1995, 'Fractals in biology and medicine', *Chaos, Solitons & Fractals*, vol. 6, pp. 171-201.

Hernandez-Contreras, D, Peregrina-Barreto, H, Rangel-Magdaleno, J, Ramirez-Cortes, J, Renero-Carrillo, F and Avina-Cervantes, G 2015, 'Evaluation of thermal patterns and

distribution applied to the study of diabetic foot', *2015 IEEE International Instrumentation and Measurement Technology Conference (I2MTC) Proceedings* (pp. 482-487). IEEE.

Hettiarachchi, NDJ, Mahindaratne, RBH, Mendis, GDC, Nanayakkara, HT and Nanayakkara, ND 2013, 'Mobile based wound measurement', *2013 IEEE Point-of-Care Healthcare Technologies (PHT)* (pp. 298-301). IEEE.

Houghton, VJ, Bower, VM & Chant, DC 2013, 'Is an increase in skin temperature predictive of neuropathic foot ulceration in people with diabetes? A systematic review and meta-analysis', *Journal of foot and ankle research*, vol. 6, no. 1, p. 31.

Ince, P, Game, FL & Jeffcoate, WJ 2007, 'Rate of healing of neuropathic ulcers of the foot in diabetes and its relationship to ulcer duration and ulcer area', *Diabetes care*, vol. 30, no. 3, pp. 660-663.

Iraj, B, Khorvash, F, Ebneshahidi, A & Askari, G 2013, 'Prevention of diabetic foot ulcer', *International journal of preventive medicine*, vol. 4, no. 3, p. 373.

Jayalalitha, G and Uthayakumar, R 2007, 'Estimating the skin Cancer using fractals', *International Conference on Computational Intelligence and Multimedia Applications (ICCIMA 2007)* (Vol. 2, pp. 306-311). IEEE.

Jeffcoate, WJ 2012, 'Wound healing–a practical algorithm', *Diabetes/metabolism research and reviews*, vol. 28, pp. 85-88.

Jones, J, Barr, W, Robinson, J & Carlisle, C 2006, 'Depression in patients with chronic venous ulceration.', *British Journal of Nursing*, vol. 15, no. 11, pp. S17-S23.

Josso, B, Burton, DR & Lalor, MJ 2002, 'Frequency normalised wavelet transform for surface roughness analysis and characterisation', *Wear*, vol. 252, no. 5-6, pp. 491-500.

Kaabouch, N, Hu, W-C, Chen, Y, Anderson, JW, Ames, F & Paulson, R 2010, 'Predicting neuropathic ulceration: analysis of static temperature distributions in thermal images', *Journal of biomedical optics*, vol. 15, no. 6, p. 061715.

Kass, M, Witkin, A & Terzopoulos, D 1988, 'Snakes: Active contour models', *International journal of computer vision*, vol. 1, no. 4, pp. 321-331.

Khaodhiar, L, Dinh, T, Schomacker, KT, Panasyuk, SV, Freeman, JE, Lew, R, Vo, T, Panasyuk, AA, Lima, C & Giurini, JM 2007, 'The use of medical hyperspectral technology to evaluate microcirculatory changes in diabetic foot ulcers and to predict clinical outcomes', *Diabetes care*, vol. 30, no. 4, pp. 903-910.

Khoo, R & Jansen, S 2016, 'The Evolving Field of Wound Measurement Techniques: A Literature Review', *Wounds: a compendium of clinical research and practice*, vol. 28, no. 6, pp. 175-181.

Kikuchi, A, Kozuma, S, Sakamaki, K, Saito, M, Marumo, G, Yasugi, T & Taketani, Y 2002, 'Fractal tumor growth of ovarian cancer: sonographic evaluation', *Gynecologic oncology*, vol. 87, no. 3, pp. 295-302.

Kranke, P, Bennett, MH, Martyn, SJM, Schnabel, A & Debus, SE 2012, 'Hyperbaric oxygen therapy for chronic wounds', *Cochrane Database of Systematic Reviews*, vol. 4.

Laing, P 1998, 'The development and complications of diabetic foot ulcers', *The American journal of surgery*, vol. 176, no. 2, pp. 11S-19S.

Landini, G & Rippin, J 1996, 'How important is tumour shape? Quantification of the epithelial–connective tissue interface in oral lesions using local connected fractal dimension analysis', *The Journal of pathology*, vol. 179, no. 2, pp. 210-217.

Lazzarini, PA, Gurr, JM, Rogers, JR, Schox, A & Bergin, SM 2012, 'Diabetes foot disease: the Cinderella of Australian diabetes management?', *Journal of foot and ankle research*, vol. 5, no. 1, p. 24.

Lee, TK, McLean, DI & Atkins, MS 2003, 'Irregularity index: a new border irregularity measure for cutaneous melanocytic lesions', *Medical image analysis*, vol. 7, no. 1, pp. 47-64.

Levey, AS, Stevens, LA, Schmid, CH, Zhang, YL, Castro, AF, 3rd, Feldman, HI, Kusek, JW, Eggers, P, Van Lente, F, Greene, T, Coresh, J & Ckd, EPI 2009, 'A new equation to estimate glomerular filtration rate', *Ann Intern Med*, vol. 150, no. 9, pp. 604-612.

Lipsky, BA, Berendt, AR, Cornia, PB, Pile, JC, Peters, EJ, Armstrong, DG, Deery, HG, Embil, JM, Joseph, WS & Karchmer, AW 2012, '2012 Infectious Diseases Society of America clinical practice guideline for the diagnosis and treatment of diabetic foot infections', *Clinical infectious diseases*, vol. 54, no. 12, pp. e132-e173.

Liu, C, van Netten, JJ, Van Baal, JG, Bus, SA & van Der Heijden, F 2015, 'Automatic detection of diabetic foot complications with infrared thermography by asymmetric analysis', *Journal of biomedical optics*, vol. 20, no. 2, p. 026003.

Losa, GA 2011, 'Fractals in biology and medicine', *Reviews in Cell Biology and Molecular Medicine*, vol.

Macdonald, A, Petrova, N, Ainarkar, S, Allen, J, Plassmann, P, Whittam, A, Bevans, J, Ring, F, Kluwe, B & Simpson, R 2016, 'Thermal symmetry of healthy feet: a precursor to a thermal study of diabetic feet prior to skin breakdown', *Physiological measurement*, vol. 38, no. 1, p. 33.

Mani, R, Romanelli, M & Shukla, V 2012, *Measurements in Wound Healing: Science and Practice*, Springer Science & Business Media.

Martinez, L 2002, 'A non-invasive spectral reflectance method for mapping blood oxygen saturation in wounds', *Applied Imagery Pattern Recognition Workshop, 2002. Proceedings.* (pp. 112-116). IEEE.

Meloni, M, Izzo, V, Giurato, L, Cervelli, V, Gandini, R & Uccioli, L 2018, 'Impact of heart failure and dialysis in the prognosis of diabetic patients with ischemic foot ulcers', *Journal of clinical & translational endocrinology*, vol. 11, p. 31.

Mendes, R, Sousa, N, Almeida, A, Vilaça-Alves, J, Reis, VM & Neves, EB 2015, 'Thermography: a technique for assessing the risk of developing diabetic foot disorders', *Postgraduate medical journal*, vol. 91, no. 1079, pp. 538-538.

Menke, NB, Ward, KR, Witten, TM, Bonchev, DG & Diegelmann, RF 2007, 'Impaired wound healing', *Clinics in dermatology*, vol. 25, no. 1, pp. 19-25.

Milne, TE, Schoen, DE, Bower, V, Burrows, SA, Westphal, C & Gurr, JM 2013, 'Healing times of diabetic foot ulcers: investigating the influence of infection and peripheral arterial disease', *J Diab Foot Complications*, vol. 5, pp. 29-38.

Moulik, PK, Mtonga, R & Gill, GV 2003, 'Amputation and mortality in new-onset diabetic foot ulcers stratified by etiology', *Diabetes care*, vol. 26, no. 2, pp. 491-494.

Mu, T, Nandi, AK & Rangayyan, RM 2008, 'Classification of breast masses using selected shape, edge-sharpness, and texture features with linear and kernel-based classifiers', *Journal of Digital Imaging*, vol. 21, no. 2, pp. 153-169.

Ndip, A & Jude, EB 2009, 'Emerging Evidence for Neuroischemic Diabetic Foot Ulcers: Model of Care and How to Adapt Practice', *The International Journal of Lower Extremity Wounds*, vol. 8, no. 2, pp. 82-94.

Nelson, EA, Cullum, N & Jones, J 2006, 'Venous leg ulcers', *Clin Evid*, vol. 15, pp. 2607-2626.

Nguyen, TM and Rangayyan, RM 2006, 'Shape analysis of breast masses in mammograms via the fractal dimension', *2005 IEEE Engineering in Medicine and Biology 27th Annual Conference* (pp. 3210-3213). IEEE.

Norman, RE, Gibb, M, Dyer, A, Prentice, J, Yelland, S, Cheng, Q, Lazzarini, PA, Carville, K, Innes-Walker, K & Finlayson, K 2016, 'Improved wound management at lower cost: a sensible goal for Australia', *International wound journal*, vol. 13, no. 3, pp. 303-316.

Nouvong, A, Hoogwerf, B, Mohler, E, Davis, B, Tajaddini, A & Medenilla, E 2009, 'Evaluation of diabetic foot ulcer healing with hyperspectral imaging of oxyhemoglobin and deoxyhemoglobin', *Diabetes care*, vol. 32, no. 11, pp. 2056-2061.

O'Meara, S, Cullum, NA & Nelson, EA 2009, 'Compression for venous leg ulcers', *Cochrane Database of Systematic Reviews*, vol. no. 1, p. CD000265.

Ogurtsova, K, da Rocha Fernandes, J, Huang, Y, Linnenkamp, U, Guariguata, L, Cho, N, Cavan, D, Shaw, J & Makaroff, L 2017, 'IDF Diabetes Atlas: Global estimates for the prevalence of diabetes for 2015 and 2040', *Diabetes research and clinical practice*, vol. 128, pp. 40-50.

Otte, J, van Netten, JJ & Woittiez, A-JJ 2015, 'The association of chronic kidney disease and dialysis treatment with foot ulceration and major amputation', *Journal of vascular surgery*, vol. 62, no. 2, pp. 406-411.

Paul, DW, Ghassemi, P, Ramella-Roman, JC, Prindeze, NJ, Moffatt, LT, Alkhalil, A & Shupp, JW 2015, 'Noninvasive imaging technologies for cutaneous wound assessment: a review', *Wound Repair and Regeneration*, vol. 23, no. 2, pp. 149-162.

Pavlovčič, U, Diaci, J, Možina, J & Jezeršek, M 2015, 'Wound perimeter, area, and volume measurement based on laser 3D and color acquisition', *Biomedical engineering online*, vol. 14, no. 1, p. 39.

Phillips, T, Stanton, B, Provan, A & Lew, R 1994, 'A study of the impact of leg ulcers on quality of life: financial, social, and psychological implications.', *Journal of the American Academy of Dermatology*, vol. 31, pp. 49-53.

Piaggesi, A, Schipani, E, Campi, F, Romanelliz, M, Baccetti, F, Arvia, C & Navalesi, R 1998, 'Neuropathic Foot Ulcers: a Randomized Trial', *Diabet. Med*, vol. 15, pp. 412-417.

Piantanelli, A, Maponi, P, Scalise, L, Serresi, S, Cialabrini, A & Basso, A 2005, 'Fractal characterisation of boundary irregularity in skin pigmented lesions', *Medical and Biological Engineering and Computing*, vol. 43, no. 4, pp. 436-442.

Pohlman, S, Powell, KA, Obuchowski, NA, Chilcote, WA & Grundfest-Broniatowski, S 1996, 'Quantitative classification of breast tumors in digitized mammograms', *Medical Physics*, vol. 23, no. 8, pp. 1337-1345.

Pradhan, S & Kariyappa, M 2016, 'Infrared Thermal Imaging for Interpreting Complications of Diabetic Foot Ulcers: A Case Control Study', *International Journal of Contemporary Medical Research*, vol. 3, no. 9, pp. 2757-2759.

Price, PE, Fagervik-Morton, H, Mudge, EJ, Beele, H, Ruiz, JC, Nystrøm, TH, Lindholm, C, Maume, S, Melby-Østergaard, B, Peter, Y, Romanelli, M, Seppänen, S, Serena, TE, Sibbald, G, Soriano, JV, White, W, Wollina, U, Woo, KY, Wyndham-White, C & Harding, KG 2008, 'Dressing-related pain in patients with chronic wounds: an international patient perspective', *International wound journal*, vol. 5, no. 2, pp. 159-171.

Rabe, E & Pannier, F 2012, 'Clinical, aetiological, anatomical and pathological classification (CEAP): gold standard and limits', *Phlebology*, vol. 27, no. 1_suppl, pp. 114-118.

Raguso, G, Ancona, A, Chieppa, L, L'Abbate, S, Pepe, ML, Mangieri, F, De Palo, M and Rangayyan, RM 2010, 'Application of fractal analysis to mammography', *2010 Annual International Conference of the IEEE Engineering in Medicine and Biology* (pp. 3182-3185). IEEE.

Rahmati, P, Adler, A & Hamarneh, G 2012, 'Mammography segmentation with maximum likelihood active contours', *Medical image analysis*, vol. 16, no. 6, pp. 1167-1186.

Ramsey, SD, Newton, K, Blough, D, Mcculloch, DK, Sandhu, N, Reiber, GE & Wagner, EH 1999, 'Incidence, outcomes, and cost of foot ulcers in patients with diabetes', *Diabetes care*, vol. 22, no. 3, pp. 382-387.

Rangayyan, RM & Nguyen, TM 2007, 'Fractal analysis of contours of breast masses in mammograms', *Journal of Digital Imaging*, vol. 20, no. 3, pp. 223-237.

Rani, P, Aliahmad, B and Kumar, DK 2017, 'A novel approach for quantification of contour irregularities of diabetic foot ulcers and its association with ischemic heart disease', *2017 39th Annual International Conference of the IEEE Engineering in Medicine and Biology Society (EMBC)* (pp. 1437-1440). IEEE.

Rani, P, Aliahmad, B & Kumar, DK 2019, 'Curve irregularity index for quantification of roughness in non-fractal curves', *Physica A: Statistical Mechanics and its Applications*, vol. 528, p. 121435.

Rani, P, Aliahmad, B and Kumar, DK 2019, 'The Association of temperature of Diabetic Foot Ulcers with Chronic Kidney Disorder', *2019 IEEE Engineering in Medicine and Biology Society (EMBC)*.

Reiber, GE, Vileikyte, L, Boyko, Ed, Del Aguila, M, Smith, DG, Lavery, LA & Boulton, A 1999, 'Causal pathways for incident lower-extremity ulcers in patients with diabetes from two settings', *Diabetes care*, vol. 22, no. 1, pp. 157-162.

Ribu, L, Hanestad, BR, Moum, T, Birkeland, K & Rustoen, T 2007, 'A comparison of the health-related quality of life in patients with diabetic foot ulcers, with a diabetes group and a nondiabetes group from the general population', *Quality of Life Research*, vol. 16, no. 2, pp. 179-189.

Ring, F 2010, *Thermal imaging today and its relevance to diabetes*, SAGE Publications, 1932-2968.

Rowledge, A, Frescos, N, Miller, C, Perry, E & McGuiness, W 2016, 'The diabetic foot ulcer periwound: a comparison of visual assessment and a skin diagnostic device', *Wound Practice & Research: Journal of the Australian Wound Management Association*, vol. 24, no. 3, p. 160.

Savage, PEA 2012, *Problems in peripheral vascular disease*, Springer Science & Business Media.

Seah, J, Yao, H, MacIsaac, R, Ekinci, E and Jerums, G 2014, 'Reducing the complications of type 2 diabetes: challenges in individualising care', *Medicine Today*, *15*(3), pp.37-47.

Shearman, C 2015, *Management of Diabetic Foot Complications*, Springer London, <https://books.google.com.au/books?id=gFeEBgAAQBAJ>.

Shearman, CP 2015, 'Foot Complications in Diabetes: The Problem', in *Management of Diabetic Foot Complications*, Springer, pp. 1-7.

Sheehan, P, Jones, P, Caselli, A, Giurini, JM & Veves, A 2003, 'Percent change in wound area of diabetic foot ulcers over a 4-week period is a robust predictor of complete healing in a 12-week prospective trial', *Diabetes care*, vol. 26, no. 6, pp. 1879-1882.

Shelberg, MC, Moellering, H & Lam, N 1982, *Measuring the fractal dimensions of empirical cartographic curves*.

Smith-Strøm, H, Iversen, MM, Igland, J, Østbye, T, Graue, M, Skeie, S, Wu, B & Rokne, B 2017, 'Severity and duration of diabetic foot ulcer (DFU) before seeking care as predictors of healing time: A retrospective cohort study', *PloS one*, vol. 12, no. 5, p. e0177176.

Stamatas, GN & Kollias, N 2007, 'In vivo documentation of cutaneous inflammation using spectral imaging', *Journal of biomedical optics*, vol. 12, no. 5, pp. 051603-051603-051607.

Tesfaye, S, Boulton, AJ, Dyck, PJ, Freeman, R, Horowitz, M, Kempler, P, Lauria, G, Malik, RA, Spallone, V & Vinik, A 2010, 'Diabetic neuropathies: update on definitions, diagnostic criteria, estimation of severity, and treatments', *Diabetes care*, vol. 33, no. 10, pp. 2285-2293.

Trabelsi, O, Tlig, L, Sayadi, M and Fnaiech, F 2013, 'Skin disease analysis and tracking based on image segmentation', *2013 International Conference on Electrical Engineering and Software Applications* (pp. 1-7). IEEE.

Tresierra-Ayala, M & Rojas, AG 2017, 'Association between peripheral arterial disease and diabetic foot ulcers in patients with diabetes mellitus type 2', *Medicina Universitaria*, vol. 19, no. 76, pp. 123-126.

van Netten, JJ, van Baal, JG, Liu, C, van Der Heijden, F & Bus, SA 2013, *Infrared thermal imaging for automated detection of diabetic foot complications*, SAGE Publications Sage CA: Los Angeles, CA, 1932-2968.

Vo-Dinh, T 2004, 'A hyperspectral imaging system for in vivo optical diagnostics', *IEEE Engineering in Medicine and Biology Magazine*, vol. 23, no. 5, pp. 40-49.

Wagner, FW, Jr. 1987, 'The diabetic foot', *Orthopedics*, vol. 10, no. 1, pp. 163-172.

Warriner, RA, Snyder, RJ & Cardinal, MH 2011, 'Differentiating diabetic foot ulcers that are unlikely to heal by 12 weeks following achieving 50% percent area reduction at 4 weeks', *International wound journal*, vol. 8, no. 6, pp. 632-637.

Wei, L, Fwa, TF and Zhe, Z 2002, 'Pavement roughness analysis using wavelet theory', *In Proceedings from the 6th International Conference on Managing Pavements. Queensland, Australia*.

Woo, KY, Harding, K, Price, P & Sibbald, G 2008, 'Minimising wound-related pain at dressing change: evidence-informed practice', *International wound journal*, vol. 5, no. 2, pp. 144-157.

Wu, Y, Hou, W & Wu, S 2011, 'Brain MRI segmentation using KFCM and Chan-Vese model', *Transactions of Tianjin University*, vol. 17, no. 3, pp. 215-219.

Yang, XS & Papa, JP 2016, *Bio-Inspired Computation and Applications in Image Processing*, Elsevier Science, <https://books.google.com.au/books?id=mvmqCgAAQBAJ>.

Yazdanpanah, L, Nasiri, M & Adarvishi, S 2015, 'Literature review on the management of diabetic foot ulcer', *World journal of diabetes*, vol. 6, no. 1, pp. 37-53.

Ylitalo, KR, Sowers, M & Heeringa, S 2011, 'Peripheral Vascular Disease and Peripheral Neuropathy in Individuals With Cardiometabolic Clustering and Obesity: National Health and Nutrition Examination Survey 2001–2004', *Diabetes care*, vol. 34, no. 7, pp. 1642-1647.

Yotsu, RR, Pham, NM, Oe, M, Nagase, T, Sanada, H, Hara, H, Fukuda, S, Fujitani, J, Yamamoto-Honda, R & Kajio, H 2014, 'Comparison of characteristics and healing course of diabetic foot ulcers by etiological classification: neuropathic, ischemic, and neuro-ischemic type', *Journal of Diabetes and its Complications*, vol. 28, no. 4, pp. 528-535.

Yudovsky, D, Nouvong, A & Pilon, L 2010, 'Hyperspectral imaging in diabetic foot wound care', *Journal of diabetes science and technology*, vol. 4, no. 5, pp. 1099-1113.

Zimny, S, Schatz, H & Pfohl, M 2002, 'Determinants and estimation of healing times in diabetic foot ulcers', *Journal of Diabetes and its Complications*, vol. 16, no. 5, pp. 327-332.